Experimental Cell Research 441 (2024) 114155

Contents lists available at ScienceDirect

Experimental Cell Research

journal homepage: www.elsevier.com/locate/yexcr

Research article

# Ascites microenvironment conditions the peritoneal pre-metastatic niche to promote the implantation of ovarian tumor spheroids: Involvement of fibrinogen/fibrin and αV and α5β1 integrins

Carine Laurent-Issartel [a], Alexandra Landras [a], Rémy Agniel [a], Florence Giffard [b,d,e], Cécile Blanc-Fournier [b,c], Elisabete Da Silva Cruz [f], Chahrazed Habes [a], Johanne Leroy-Dudal [a], Franck Carreiras [a,1], Sabrina Kellouche [a,*,1]

[a] Equipe de Recherche sur Les Relations Matrice Extracellulaire-Cellules, ERRMECe, (EA1391), Groupe Matrice Extracellulaire et Physiopathologie (MECuP), Institut des Materiaux, I-MAT (FD4122), CY Cergy Paris Université, France
[b] UNICANCER, F. Baclesse Comprehensive Cancer Center, Biopathology Department, Caen, France
[c] Université de Caen Normandie, Unité de Services PLATON, Centre de Ressources Biologiques OvaRessources, Caen, France
[d] Université de Caen Normandie, Inserm U1086 ANTICIPE, Caen, France
[e] Université de Caen Normandie, Unité de Services PLATON, Plateforme Virtual'His, Caen, France
[f] University of Strasbourg, Laboratory of Bioimaging and Pathologies, UMR CNRS 7021, Illkirch, France

ARTICLE INFO

*Keywords:*
Ascites
Ovarian tumor spheroids
Mesothelium integrity
Fibrinogen/fibrin
αV / α5β1 integrins
3D co-culture

ABSTRACT

At least one-third of patients with epithelial ovarian cancer (OC) present ascites at diagnosis and almost all have ascites at recurrence especially because of the propensity of the OC cells to spread in the abdominal cavity leading to peritoneal metastasis. The influence of ascites on the development of pre-metastatic niches, and on the biological mechanisms leading to cancer cell colonization of the mesothelium, remains poorly understood.

Here, we show that ascites weakens the mesothelium by affecting the morphology of mesothelial cells and by destabilizing their distribution in the cell cycle. Ascites also causes destabilization of the integrity of mesothelium by modifying the organization of cell junctions, but it does not affect the synthesis of N-cadherin and ZO-1 by mesothelial cells. Moreover, ascites induces disorganization of focal contacts and causes actin cytoskeletal reorganization potentially dependent on the activity of Rac1. Ascites allows the densification and reorganization of ECM proteins of the mesothelium, especially fibrinogen/fibrin, and indicates that it is a source of the fibrinogen and fibrin surrounding OC spheroids. The fibrin in ascites leads to the adhesion of OC spheroids to the mesothelium, and ascites promotes their disaggregation followed by the clearance of mesothelial cells. Both αV and α5β1 integrins are involved.

In conclusion ascites and its fibrinogen/fibrin composition affects the integrity of the mesothelium and promotes the integrin-dependent implantation of OC spheroids in the mesothelium.

## 1. Background

Ovarian cancer is the gynecological malignancy with the highest case-to-mortality ratio in the Western world. Because ovarian cancer is often asymptomatic, it is generally diagnosed at an advanced stage and is associated with a poor prognosis (5-year survival rate ~30 %) mainly due to acquired chemoresistance and widespread dissemination [1]. Ovarian carcinoma metastasizes by continuous infiltration of neighboring organs and disseminates within the peritoneal fluid of the abdominal cavity. Ovarian metastasis is commonly due to the shedding of individual tumor cells or free-floating multicellular clusters, spheroids, from the primary tumor into the abdominal cavity, where they survive and subsequently spread after attachment to the peritoneum. Once attached to the mesothelial layer of the peritoneum, malignant cells proliferate, invade it and metastasize to distant organs [2–5].

At least one-third of patients with epithelial ovarian cancer present ascites, an exudative fluid that accumulates intra-abdominally, at diagnosis. Almost all patients have ascites at recurrence especially

* Corresponding author.
*E-mail address:* sabrina.kellouche@cyu.fr (S. Kellouche).
[1] These authors contributed equally to this work.

https://doi.org/10.1016/j.yexcr.2024.114155
Received 15 February 2024; Received in revised form 5 July 2024; Accepted 9 July 2024
Available online 14 July 2024

because of the propensity of the malignant cells to spread in the abdominal cavity and develop chemoresistance [6]. The presence of a large volume of ascites correlates with poor prognosis, and transcoelomic metastasis (through the mesothelium) seems to be directly associated with ascites production. Indeed, reduction in peritoneal tumor bulk as a result of surgery and chemotherapy is generally associated with a reduction of ascites production [6,7]. Ascites fluid is a dynamic reservoir of survival factors owing to its large content of many different molecules, such as cytokines, growth factors, angiogenic factors, hormones, coagulation factors, proteases and extracellular matrix (ECM) proteins that individually and/or collectively affect cancer cell adhesion, migration, invasion, survival and spheroid formation [8–10]. Since ascites represents a unique tumor microenvironment, its effects remain to be fully characterized, especially regarding the regulation of malignant spheroid cell dissemination.

Ovarian carcinoma dissemination is partly due to the formation of spheroids that are released within the peritoneal cavity before implantation into the mesothelium. The multicellular nature of spheroids is thought to be attributable to adhesive molecules that mediate cell-cell and cell-ECM interactions. Among secreted ECM, fibronectin promotes the formation of spheroids, and is associated with their increased expression of α3β1, α4β1 and α5β1 integrins [11,12]. Other studies show the importance of vitronectin and its αv integrin receptors in the early stages of spheroid formation [12]. In addition, these cell-ECM interactions lead to signals that could regulate spheroid cell behavior, such as resistance to anoikis [9,13]. Spheroids can become chemoresistant. The first reason is that the three-dimensional organization of the spheroids results in poor delivery of chemotherapeutic drugs to the inner regions of spheroids [14]. The low rate of cancer cell proliferation in spheroids could be one of the reasons for the loss of sensitivity to therapeutic agents targeting the cell cycle.

Interestingly, unlike most other cancers, ovarian tumors rarely disseminate through the blood vessels. Cells spread predominantly by direct extension of the tumor into adjacent tissues, and by the shedding of cancer cells from the primary tumor into the peritoneal cavity. Thus, ovarian cancer cells are preferentially found as a solid tumor mass adhering to the peritoneal mesothelium [15]. The mesothelium, a single layer of flat cells covering the peritoneal cavity and its organs, is the first barrier met by ovarian tumor cells and is the major site of ovarian carcinoma metastasis before invading the underlying connective tissue. Mesothelial cells express and/or secrete several extracellular matrix proteins, adhesion molecules and chemotactic factors that could enhance ovarian cancer cell implantation and colonization of the mesothelium [2,16–18]. Thus, mesothelial cells and the ECM constituting the implantation site of ovarian tumors act as a propitious microenvironment for tumor growth. Both cancer cells and ascites can induce changes in the surrounding mesothelial microenvironment, creating the so-called “reactive tumor microenvironment”.

Mesothelial cells do not synthesize fibrinogen, although accumulation of fibrinogen in tumor ascites has been previously identified. Fibrinogen is a coagulation protein found in blood plasma that increases its levels in inflammatory conditions such as ovarian cancer [19]. Fibrinogen and its polymerized form fibrin are also regular components of solid tumor stroma. Indeed, the process of wound healing or tumor induces a decrease in oxygen level which causes the tissue or tumor to be hypoxic. To compensate this lack, the tissue responds by expressing proteins involved in coagulation and fibrinolysis [20]. In addition, in response to the activation of the immune system, the clotting pathway is also induced to counteract the tumor giving a pro-coagulant [21] tumor phenotype. *In vivo* experiments in mice have shown the presence of fibrin deposition on the surface of the peritoneal cavity after implantation of ovarian cancer cells [22,23–25]. These data led us to explore the potential involvement of ascites-derived fibrinogen/fibrin in producing a propitious microenvironment for the implantation and dissemination of ovarian carcinoma in the peritoneal mesothelium.

Thus, we determined the influence of ascites on ovarian cancer spheroid implantation and dissemination in the peritoneal mesothelium. To mimic the early stages of peritoneal implantation of ovarian cancer, we developed an *in vitro* three-dimensional model of co-culture of tumor spheroids and healthy mesothelial cells in the presence of ascites. In particular, we explored the impact of ascites and its components on: i) the integrity of the peritoneal mesothelium, ii) the ability of ovarian cancer cells to form spheroids, and iii) the implantation of spheroids within mesothelial cell monolayers and their clearance due to spheroid spreading.

## 2. Methods

### 2.1. Ascites samples

The ascites samples were collected after obtaining informed consent from patients with serous high-grade ovarian cancer at the F. Baclesse Cancer Center (Caen, France). The ascites samples were certified cytologically as positive for malignant cells (Supplementary Table 1) and stored in the OvaRessources Biological Resources Center (BRC) (NF–S 96900 quality management, AFNOR N°2016:72860.5). The Medical Officer and the Scientific Officer of the BRC are respectively Dr Cécile Blanc Fournier and Dr Laurent Poulain. All biological collection from BRC was declared by the Project Manager of the Clinical Research Department (Alexandra Leconte) to the French Ministry of Education, Health and Research (MESR) (N°DC-2010-1243 and amendments DC-2013-1849, DC-2016-2641 and DC-2017-2923). The collection of samples was approved on 17 September 2011. The study was approved by the CPP North West III ethical committee (Committee for the Protection of Persons). Immediately after collection, the ascites samples were centrifuged at 400 g for 5 min immediately after collection to remove malignant and blood cells, and the supernatants stored at −20 °C. The acellular fraction of ascites samples was sterilized by filtration (0.2 μm, low-binding) and supplemented with penicillin (200 UI/mL)/streptomycin (200 μg/ml) before cell culturing. The ascites were macroscopically heterogeneous and differed according to their opacity, viscosity/gelatinous appearance (filtration difficulties) and hematogenous properties. We used 8 ascites from 8 patients, which were labeled ASC#1 through ASC#8 (Supplementary Table 1).

### 2.2. Cells and reagents

The human ovarian adenocarcinoma cell lines, SKOV3 (American Type Culture Collection, Manassas, USA (ATCC), HTB-79) and OVCAR3 (ATCC HTB-161), were kindly supplied by Dr L. Poulain of the BioTICLA team INSERM U1086 (Biologie et Thérapie Innovantes des Cancers Localement Agressifs, Caen, France). Both ovarian cancer cell lines derived from malignant ascites of serous ovarian adenocarcinoma. The cells were grown in RPMI-1640 glutaMAX (Life Technologies, France) containing 0.07 % (v/v) sodium bicarbonate supplemented with 10 % fetal bovine serum (FBS, Biosera, France) in a humidified air atmosphere with 5 % $CO_2$ in air at 37 °C. Normal human peritoneal mesothelial cells strain LP-9 derived from ascites fluid of the peritoneal cavity of an ovarian cancer patient were purchased from Coriell Institute (AG07086, New Jersey, US). LP-9 cells were grown in Medium M199 and HAMF12 (1:1 mixture) containing 10 ng/ml epidermal growth factor (EGF; Sigma St-Quentin-Fallavier, France), 0.4 μg/ml hydrocortisone (Sigma), 1 % penicillin/streptomycin supplemented with 15 % FBS. The human mesothelial cell lines, Met-5A-CRL-94444, purchased from ATCC, were grown in M199 supplemented with 3.3 nM epidermal growth factor, 870 nM insulin, 400 nM hydrocortisone, 1.25 g/L sodium bicarbonate (Invitrogen) and 10 % FBS. The mesothelial origin of Met-5A and LP-9 cells was confirmed by the presence of calretinin, a specific marker on the cells, as revealed by immunostaining (Supplementary Fig. S1). The cultured cells were in a humidified atmosphere of 5 % $CO_2$ in air at 37 °C. Sub-confluent cells were harvested with 0.25 % trypsin-EDTA (Life Technologies, France). In some experiments, cells were cultured

on 10 μg/ml fibronectin, vitronectin or fibrinogen coatings. Fibronectin and vitronectin were purified from human blood plasma (provided by the French Establishment of Blood), as described by Poulain et al. [10, 26]. Fibrinogen was purchased from Hyphen BioMed (PP001C).

### 2.3. Cell viability assay

To mimic the mesothelium, Met-5A or LP9 cells were seeded in 24-well plates at 16,000/cm$^2$ and incubated in complete M199 medium or M199/HAMF12 respectively (named growth medium, GM) for 5 days until confluent. The medium was then removed and cells were incubated in new growth medium or ascites (#1, #2, #6 or #7). All experiments were carried out in 100 % ascites in order to be close to the pathological reality where mesothelial and ovarian cancer cells are in contact with the ascites microenvironment accumulated in the peritoneal cavity of ovarian cancer patients. The number of mesothelial viable cells was measured by the trypan-blue exclusion test at 0, 24, 72 and 96 h after the refresh of growth medium or ascites. Results are representative of 3 independent experiments done in triplicate and are expressed as mean ± Standard Error of the Mean (SEM).

### 2.4. Cell cycle analysis

Met-5A cells were seeded in culture flask (75 cm$^2$) and incubated in growth medium for 5 days until confluent. The cells were then incubated in new growth medium or ascites (#1, #2 or #6) for 24 or 96 h. Cells were rinsed twice with phosphate buffer saline (PBS), harvested with trypsin-EDTA and resuspended in growth medium. After centrifugation, cells were fixed in 70 % ethanol and stored at −20 °C overnight. After centrifugation, cells were resuspended in PBS Ca+2 Mg + 2 and with RNase (40 μg/ml) (AM2694, INVITROGEN). Cells were stained in ice for 30 min with propidium iodide (20 μg/ml) (P4864, Sigma-Aldrich). Cells (50,000) were analyzed per condition in a flow cytometer (BD Accuri C6plus). The percentage distribution in the Go/G1, S and G2/M phases were determined with BD Accuri C6 Plus Software.

### 2.5. Spheroid formation

Ovarian cancer spheroids were generated by the hanging-drop technique adapted from Ramsy Foty [27]. Briefly, a suspension of 500 SKOV3 or OVCAR3 cells was seeded in a total volume of 20 μL ascites. The drops containing ascites and cells were deposited on the bottom of the Petri dish; the lower part of the dish was filled with PBS and observed each day by phase-contrast microscopy, being a humid chamber that prevented evaporation of the cell-containing drops. There were at least 25 drops per dish. The lid of the Petri dish was turned upside down and placed on the bottom. The whole set was transferred to a humidified incubator at 37 °C for 5 days to help with the sedimentation and aggregation of the cells and promote the formation of 3D-ovarian cancer spheroids. Spheroid formation was monitored each day by phase-contrast microscopy, and those generated were used in the experiments described below.

### 2.6. Co-culture model

To mimic cancer cell dissemination on to a mesothelium, a co-culture assay of ovarian cancer spheroids and mesothelial cells was used. Mesothelial cells were first grown on glass coverslips in 24-well plates at 16,000/cm$^2$ for 5 days in growth medium until confluent. The spheroids formed were deposited on the mesothelial monolayer in complete medium or ascites. This model of co-culture was examined several times and used at different stages as described below.

### 2.7. Immunofluorescent staining

Met-5A or LP-9 cells seeded onto glass coverslips or co-cultured with spheroids were exposed to different ascites or growth medium at different times. At each time point, cells were fixed in 3 % paraformaldehyde (PFA) in PBS and saturated with PBS containing 0.5 % BSA for 30 min. They were permeabilized with 0.1 % Triton X100 in PBS. They were incubated for 2 h at room temperature (RT) with primary antibodies Collagen IV (C1926, Sigma-Aldrich), Fibronectin (F3648, Sigma-Aldrich), Laminin (L9393, Sigma-Aldrich), Vinculin (V9131, Sigma-Aldrich), Tubulin (T9026, Sigma-Aldrich), Vimentin (CBL202, Sigma-Aldrich), Paxillin (ab32115, Abcam), Fibrinogen (A0080, DAKO), N-Cadherin (ab45139, Abcam), ZO-1 (610966, BD Biosciences), Rho A (sc-418, Santa-Cruz), cdc42 (sc-8401, Santa-Cruz), Calretinin (M7245, Agilent) or Rac1 (610651, BD Transduction Laboratories). After washing, the coverslips were incubated with the appropriate fluorescent secondary antibodies for 1 h at RT: Alexa Fluor 568-conjugated anti-Mouse antibody (A11004, Life Technologies), Alexa Fluor 568-conjugated anti-Rabbit antibody (A11011, Life Technologies), Alexa Fluor 488-conjugated anti-Mouse antibody (A11029, Life Technologies) or Alexa Fluor 488-conjugated anti-Rabbit antibody (A11008, Life Technologies). The actin cytoskeleton was stained with FITC-phalloidin (P5282, Sigma Aldrich) or TRITC-phalloidin (P1981, Sigma Aldrich). Cell nuclei were stained with Hoechst (33342, Abcam) or DAPI (4,6-diamidino-2-phenylindole dihydrochloride, D9542, Sigma Aldrich). Coverslips were mounted in Prolong-Gold Antifade Reagent (P36930, Invitrogen). For the spheroids, the staining was carried out according to the same protocol, but in Ependorff tubes for centrifugation at each rinsing step. Moreover, spheroids were incubated overnight at 4 °C with the primary antibody, Fibrinogen (A0080, DAKO), and after washing they were incubated for 2 h at RT with the secondary antibody Alexa Fluor 488-conjugated anti-Rabbit antibody. Controls in which primary antibodies were replaced with PBS were negative. Immunofluorescent labeling was observed with a confocal microscope (LSM710, Zeiss) or an upright (DMLB, Leica) and an inverted (DMi 8 Thunder, Leica) fluorescence wide-field microscope.

### 2.8. Immunohistochemistry staining

Spheroids isolated from patient ascites were collected during surgery or ascites punctures performed on human ovarian carcinoma patients observed in the F. Baclesse Comprehensive Cancer Center (Caen, France) after certified pathological diagnosis. Paraffin-embedded sections (5 μM) were dewaxed and rehydrated, heated for 30 min at 97 °C in 10 mM citrate buffer, pH 6 for antigen retrieval, washed with 0.1 M Tris–0.15 M NaCl and incubated with 10 % hydrogen peroxide to block endogenous peroxidase activity. Non-specific sites of fixation were saturated with a neutralizing solution from an Ultratech HRP kit. The sections were incubated for 1 h at RT with an anti-fibrinogen antibody (1:400) (A0080, DAKO). After PBS washing, the sections were incubated with the Ultratech HRP Streptavidin-Biotin Universal Detection System (Beckman Coulter, Villepinte, France). Staining was visualized using a DAB chromogen system (Zymed, Clinisciences, Montrouge, France) and nuclei were counterstained with hematoxylin. After washing with water, the sections were dehydrated in alcohol and toluene before being mounted with Entellan (Merck, Darmstadt, Germany). The primary antibody was omitted from the negative controls. The xenografts of ovarian cancer cells injected into the peritoneum of nude mice led to the development of peritoneal carcinomatosis according to Ref. [28]. Female Swiss nude mice/4-week-old mice were obtained from Charles-River Laboratories (L'Abresles, France) and maintained in a pathogen-free environment. Each of the 6-8-week-old animals was implanted intraperitoneally with 2 × 10$^7$ ovarian adenocarcinoma SKOV3 cells and inspected and weighed daily. During the carcinomatosis characterization experiment, three mice were killed and dissected on days 7, 14, 21, and 28; the others were killed and autopsied when considered as moribund. Organs and tumors were fixed in formalin and paraffin-embedded for histological examination.

Mesothelium slices of the xenografts were treated with a fibrinogen

IHC, as previously described, after being removed on day 28. For the negative controls, the primary antibody was omitted from the tumor slice.

### 2.9. Scanning electron microscope

The samples analyzed by SEM (GeminiSEM 300, Zeiss) were treated as follows: the growth medium was removed by rinsing twice with warmed PBS (37 °C) and a suspension for dehydration with 0.2 M cacodylate and 2 % glutaraldehyde was added for 30 min at RT. The samples were rinsed 3 times with 0.2 M cacodylate and successively placed in different baths of 30, 50, 80 and 100 % ethanol for 10 min each. Samples were critical-point dried for 16 exchanges (EM CPD300, Leica). Finally, they were sputter-coated with a thin layer of platinum (4 nm), before being imaged in the SEM.

### 2.10. Correlative Light-Electron Microscopy

Met-5A cells were seeded on glass coverslips with a grid pattern (P35G-1.5-14-CGRD, MatTek) and incubated in growth medium until confluent. The cells were then incubated in ascites. After 24 h incubation, cells were fixed in 3 % paraformaldehyde (PFA) in PBS and saturated with PBS containing 0.5 % BSA for 30 min. They were permeabilized with 0.1 % Triton X100 in PBS. They were incubated for 2 h at RT with the primary antibody: Fibrinogen (A0080, DAKO). After washing, the coverslips were incubated with the appropriate fluorescent secondary antibodies for 1 h at RT: Alexa Fluor 488-conjugated anti-Rabbit antibody (A11008, Life Technologies). Coverslips were left in PBS and immunofluorescent labeling examined with a confocal microscope (LSM710, Zeiss). The cells were then washed, dehydrated and dried as previously described. Finally, cells were sputter-coated with 4 nm platinum before being observed in the SEM. Confocal microscope and SEM acquisitions were superimposed with ICY, the open source image processing software, using the ecCLEM plugin [29].

### 2.11. Quantification of ascitic fibrinogen and thrombin

Human fibrinogen and thrombin concentrations were measured using sensitive immunoassay kits (ab208036, ab108909, Abcam, respectively). Antibodies specific to the protein being examined had been fixed on 96-well plates. Standard samples for the calibration range, the culture medium and ascites samples were deposited on the wells at predetermined dilutions; each sample was assayed in duplicate. Protein-specific biotinylated detection antibodies were added, followed by several rinses. TMB (3,3′,5,5′-tetramethylbenzidine) was used to visualize the streptavidin-peroxidase enzymatic reaction. Streptavidin-peroxidase specifically catalyzes TMB to produce a blue product that turns yellow after adding a stop solution. The absorbance was measured at 450 nm by the spectrofluorometer (Xenius XM, SAFAS). Fibrinogen and thrombin concentrations were determined from the calibration curve of the corresponding standards.

### 2.12. Western blotting

Having been previously determined using the BiCinchoninic Acid Assay (BSA) (BCA1-1 KT, Sigma-Aldrich), equal amounts of the different ascites and complete M199 culture medium (growth medium) protein (10 μg) were treated with Laemmli buffer (125 nM Tris pH 6.8, 20 % glycerol, 4 % SDS, 0.005 % bromophenol blue, 5 % β-mercaptoethanol). They were separated by 10 % bis-acrylamide SDS-PAGE electrophoresis under reducing conditions, before being transferred to a nitrocellulose membrane (Bio-Rad) for 1 h at 100 V at room temperature. The membrane was blocked 1 h with TTBS (137 mM NaCl, 20 mM Tris-HCL, pH 7.6, 0.001 % Tween) and 5 % BSA. The membrane was probed for 2 h with anti-fibrinogen (1:1,000, A0080, DAKO). After 3 washes with TTBS, the membranes were incubated for 1 h at RT in TTBS-BSA 0.5 % with an anti-rabbit horseradish peroxidase conjugated antibody (1/5,000, A6154, Sigma-Aldrich). Following 3 washes with TTBS, immunoreactivity was detected by enhanced chemiluminescence (ECL, Millipore). Proteins were identified using an ImageQuant LAS 500 (GE Healthcare Life Sciences, France).

Met-5A cells were grown in culture flasks in growth medium until confluent, before fresh growth medium or ascites was added for 24 h. Cells were washed once with ice-cold PBS and lysed with RIPA buffer (#9806, Cell Signaling TECHNOLOGY) with PMSF protease inhibitor (P7626, Sigma-Aldrich). Cell lysates were clarified by centrifugation at 10,000 g for 10 min at 4 °C, and protein concentrations were determined using the BCA assay. Equal amounts of protein (10 μg) were treated with Laemmli buffer and electrophoresed under reducing conditions, before being transferred on a nitrocellulose membrane (Bio-Rad) for 1 h at 100 V at RT. Membranes were blocked with Blocking Buffer TBS (927–50000, Odyssey) for 1 h. Membranes were probed with anti-N-cadherin (ab45139, Abcam), anti-ZO-1 (610966, BD Biosciences), anti-β-actin (A5441, Sigma-Aldrich) and anti-α-tubulin (T9026, Sigma-Aldrich) antibodies (at dilutions of 1:1000; 1:500; 1:2500 and 1:1,000, respectively). Bound antibodies were detected using fluorescent secondary antibodies (IRDye 800CW goat anti-Rabbit and IRDye 680RD goat anti-Mouse) (1/80,000). Membrane fluorescence was read by the ODDYSEY infrared imaging system (LI-COR Biosciences).

### 2.13. Activated RhoA, cdc42 and Rac1 assays

Three members of the Rho family of GTPases have been studied: RhoA, Rac1 and Cdc42. Proteins were assayed using the BK030 cytoskeleton protocol. Using sub-confluent cultures that had been serum starved (0.10 % FBS) for 18 h, cultures were incubated with ascites or growth medium for 30 min or 24 h. Briefly, at each time point, cells were washed twice with cold PBS, scraped into 500 ml lysis buffer with proteases inhibitors. After centrifugation at 10,000 g for 1 min, the supernatants were snap-frozen in liquid nitrogen. Concentrations were determined by BCA assay; 500 μg of total cell protein under different conditions were used for pull-down assays, as well as positive and negative control. Proteins were incubated with 50 μg rhotekin-RBD (rhotekin - Rho Binding Domain) for RhoA pull-down assay and 10 μg of PAK-PBD (p21 Activated Kinase I - p21Binding Domain) for Cdc42 and Rac1 pull-down assay for 1 h at 4 °C with gentle rotation. After centrifugation and rinsing, 20 μL Laemmli sample buffer was added and the samples were analyzed by SDS-PAGE (12 %). 30 μg of total protein were analyzed for quantification of the total specific small G-protein and 20 ng His-tagged small G-protein controls, in Laemmli buffer. Proteins were transferred to PVDF membranes for 45 min at 75 V. The membranes were blocked with 5 % nonfat-dry milk in TTBS for 30 min at RT with constant agitation. The membranes were probed with anti-RhoA (1:500), anti-Rac1 (1:500) or anti-Cdc42 (1:250) antibodies diluted in TTBS overnight at 4 °C with constant agitation. After washing, membranes were incubated with anti-mouse secondary antibody HRP-conjugated (GENA931, Sigma-Aldrich) diluted in TTBS (1:5000) for 1 h at room temperature with constant agitation. After washing, the protein-linked antibodies were detected by ECL (Millipore).

### 2.14. Integrin blockage in spheroid dispersion and clearance of mesothelial cells

For inhibition experiments, implantation of spheroids in protein coatings (fibronectin, fibrinogen) or clearance study, Cyclo (-RGDfc) (637851–1, Anaspec) and Cilengitide blocking peptides (SML1594, Sigma Aldrich) were used at 100 μg/ml and 50 μg/ml, respectively. The ovarian cancer spheroids were preincubated for 2 h 30 at 4 °C with one of the blocking peptides before being deposited on protein coatings or on mesothelial monolayers that had been labeled with nanoparticles. Briefly, the mesothelial monolayer was stained by nanoparticles (NPs) (biodegradable polymers loaded with cyanine dyes) that can be

homogenously endocytosed by living cells [30]. NPs were provided to us by Dr. Andreas Reisch. For labeling, mesothelial cells were seeded in 6-well plates at 21,000/cm$^2$. After 18 h adhesion, the culture medium was removed before the cells were washed twice with PBS and once with opti-MEM (Gibco). Cells were incubated with a freshly prepared solution of the NPs. NP solution was prepared from the stock solution in 20 × $10^{-3}$ M phosphate buffer at pH 7.4 with a particle concentration of 3 × $10^{-9}$ M (0.04 g-1 L-polymer). This solution was diluted 10X with opti-MEM. The NP suspension was deposited on the cells for 3 h at 37 °C; the NP suspension was then removed, cells were rinsed with opti-MEM then PBS. Met-5A cells were detached with trypsin - EDTA and seeded onto glass coverslip until confluent. In the presence or absence (Ctrl) of integrins blocking peptides, the area of dispersion of the spheroids on the protein coatings, as well as the area of the clearance of the mesothelial cells illustrated by the absence of nanoparticle staining, were measured by Image J software.

### 2.15. Fibrin gel with spheroids: 3D culture model

To observe the dispersion and invasion of ovarian cancer spheroids in a fibrin gel with or without blocking peptides (described above), a suspension of fibrinogen at 3 mg/ml in PBS was produced. 1 U/ml of human thrombin was added and the fibrinogen (Fg) suspension was quickly transferred to 48-well plates (150 μl/well). Fibrin gel was incubated for 30 min at 37 °C to polymerize. A suspension with 150 μL Fg suspension at 3 mg/ml, 50 μL ascites containing ovarian cancer spheroids (preincubated or not with blocking peptides) and thrombin (1 U/ml) was added on the gel initially formed. The mixture was incubated at 37 °C to polymerize for 30 min. Complete medium or ascites was added to the wells. The dispersion, disaggregation and invasion of cancer-cell-derived spheroids in fibrin gels were observed at different times under a phase-contrast microscope.

### 2.16. Fibrinogen blocking: Real-time spheroid dispersion

Fibrinogen Binding Inhibitor Peptide (inh Fg, HY-P1507, Cliniscience) was used at 50 μM. The ovarian cancer spheroids were preincubated for 2 h at 4 °C with the blocking peptides before being deposited on mesothelial monolayers. The Fibrinogen Binding Inhibitor Peptide is non-selective between αIIbβ3 and αvβ3 [31]. The plates were then placed in the inverted (DMi 8 Thunder, Leica) fluorescence wide-field microscope live cell analysis system and incubated at 37 °C in 5 % $CO_2$. The initial photographs (t = 0) were taken 30 min after the spheroids were plated. Photographs were taken every 30 min for a total of 42 h. The results were analyzed to determine changes in the areas of the spheroids over time with Image J software. The area of the spheroids is measured at different time points by outlining them on Image J software (dotted line). Each image was normalized to the same dimensions so that the areas could be compared.

### 2.17. Statistical analyses

Figures were obtained from at least 3 independent experiments carried out in triplicate. Data were expressed as mean ± SEM. Analyses of the experiments used a paired unidirectional ANOVA test (*P < 0.05, **P < 0.01, ***P < 0.001).

## 3. Results

### 3.1. Ascites effects on the viability and cell cycle of the mesothelial cells

The mesothelium is a stable barrier under physiological conditions. The effects of ascites on mesothelium stability and integrity were measured. To mimic the mesothelium, mesothelial cells were seeded in growth medium for 5 days to achieve a confluent monolayer. The medium was removed and the cells incubated in new growth medium or ascites (#1, #2, #6 or #7). We chose these four ascites from the panel of 8 on the basis of different macroscopic factors such as their opacity or gelatinous appearance. After 24 h incubation in ascites, the mesothelial cells appeared slightly altered by the destabilization and accumulation of intracellular vesicles, which increased with time (96 h). In growth medium, monolayers seemed to be unchanged (Fig. 1a and b). Mesothelial cell viability within the monolayer was monitored by the trypan-blue exclusion test at 0, 24, 72 and 96 h after adding fresh growth medium or ascites (#1, #2, #6 or #7). After 96 h incubation, no effect of ascites was seen on the viability of LP9 cells compared to growth medium (Fig. 1c). After 24 h incubation, no effect of ascites was seen on the viability of Met-5A cells compared to growth medium. However, at 72 h ASC#1 and ASC#6 significantly inhibited the viability of Met-5A cells compared to growth medium. At the same time, ASC#2 seemed to have an intermediate effect between ASC#1/ASC#6 and growth medium on the viability of the cells. ASC#1 and ASC#6 significantly inhibited the proliferation of Met-5A cells compared to ASC#2. The differences between the 3 ascites were representative of their heterogeneity, but all ascites reduced the viability of the mesothelium cells over time (Fig. 1d). A further cell cycle analysis of Met-5A cells in monolayer was conducted after adding ascites (#1, #2 or #6) for 24 and 96 h. Unlike growth medium, ASC#6 significantly increased the percentage of cell debris and death (sub-G1 pic) over time (Fig. 1e). Furthermore, ASC#6 significantly decreased the proportion of Met-5A cells in G0/G1 and increased the G2/M phase. From 24 h incubation with ASC#1 or ASC#2, the percentage of cells in the S phase significantly decreased compared to growth medium. At 96 h, the number of cells in the G0/G1 phase also significantly decreased and cells in G2/M significantly increased compared to growth medium. These three ascites seemed to block cells in the G2/M phase of the cell cycle (Fig. 1e) and confirmed the decrease in the overall cell density seen in Fig. 1d. However, these results nevertheless show differences between ascites. Whereas ASC#1 and ASC#2 are only associated with a decrease in cell density by blocking the cell cycle in G2/M, ASC#6 – in addition to this blockage – seems more aggressive with a cytotoxic effect on the Met-5A monolayer. Ascites weakens the mesothelium by affecting the viability of mesothelial cells while destabilizing their distribution in the cell cycle.

### 3.2. Ascites destabilizes the integrity of the mesothelium

The mesothelium acts as a physiological barrier, but its destabilization facilitates the migration of cancer cells through it. The mesothelial monolayers were incubated for 24 h with growth medium or ascites. Immunofluorescent staining of N-cadherin (Cell Adhesion Molecules, CAM) and ZO-1 (tight junction protein) showed a regular junctional localization in mesothelial monolayers in growth medium conditions. But in ascites conditions, mesothelial monolayers showed marked dislocation of intercellular N-cadherin along with diffuse staining and an irregular ZO-1 expression (Fig. 2a and b). However, the amounts of N-cadherin and ZO-1 proteins observed by western blot on mesothelial cells were unaffected by the different ascites compared to growth medium (Fig. 2c and d). Ascites causes destabilization of the integrity of mesothelium with a modification of the organization of cell junctions, but does not affect the synthesis of N-cadherin and ZO-1.

Maintaining the integrity of mesothelium is due to the stability of the cell-cell junctions and the mechanical property of the cells which is conferred by their cytoskeleton and their anchoring. After 24 h incubation of mesothelial cells with ascites, the staining of tubulin (microtubules) and vimentin (intermediate filaments) did not show any effect of ascites on their organization compared to growth medium. Nevertheless, ascites led to actin cytoskeletal reorganization reflecting cell retraction. The filamentous actin organization within mesothelial cells shifted from stress fibers and cortical pattern in growth medium to diffuse and more dashed actin staining structures at the membrane periphery in the presence of ascites (Fig. 3a). However, western-blot analysis indicated that the intensities of actin bands remained

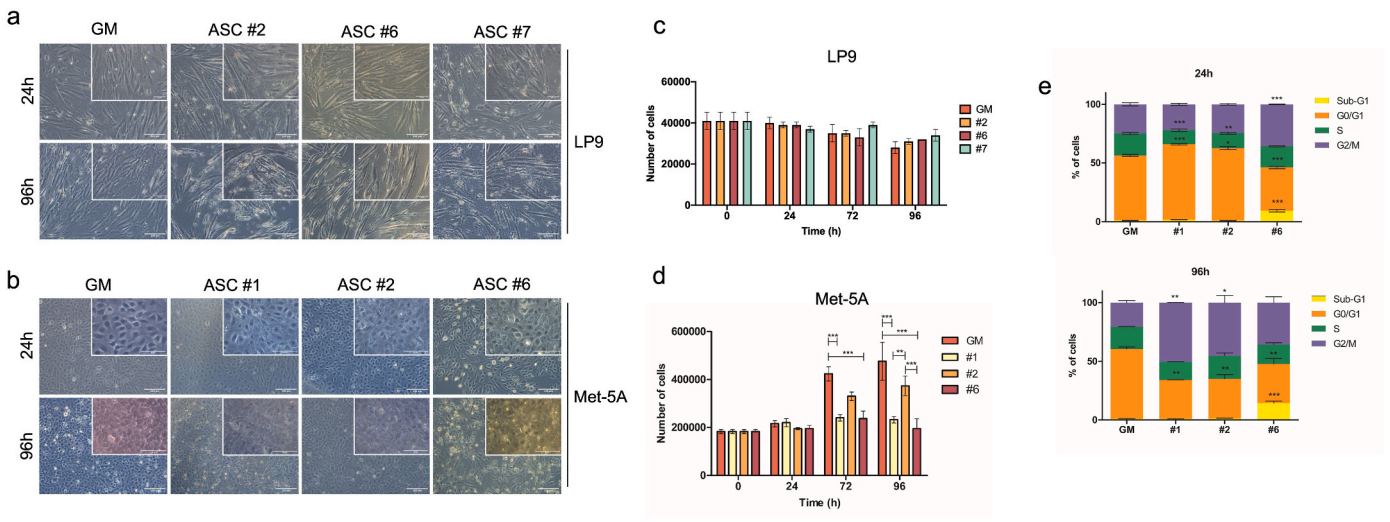


**Fig. 1.** Ascites effects on morphology and cell cycle of mesothelial cells. Confluent mesothelial monolayers were incubated with growth medium (GM) or ascites (#1, #2, #6 or #7) for 24, 72 or 96 h. Representative light micrographs were taken at 24 and 96 h for LP9 (a) or Met-5A (b). Scale bar is 100 μm and 50 μm for magnification. The number of viable cells was measured by the trypan-blue exclusion test at 24, 72 and 96 h for LP9 (c) or Met-5A (d). Results are representative of at least three independent experiments and are expressed as mean ± SEM. *P*-values were calculated by paired one-way ANOVA test (***P < 0.001) with significant differences estimated by comparing GM vs ascites. (e) Cell cycle analysis of Met-5A cells after incubated with GM or ascites for 24 or 96 h. Cells were stained with propidium iodide and analyzed in a flow cytometer. Results are representative of at least three independent experiments and are expressed as mean ± SEM. The percentage of cell cycle distribution in Sub-G1, Go/G1, S and G2/M phases were determined with BD Accuri C6 Plus Software. *P*-values were calculated by paired one-way ANOVA test (*P < 0.05, **P < 0.01, ***P < 0.001) with significant differences estimated by comparing GM vs ascites #1, #2, or #6.

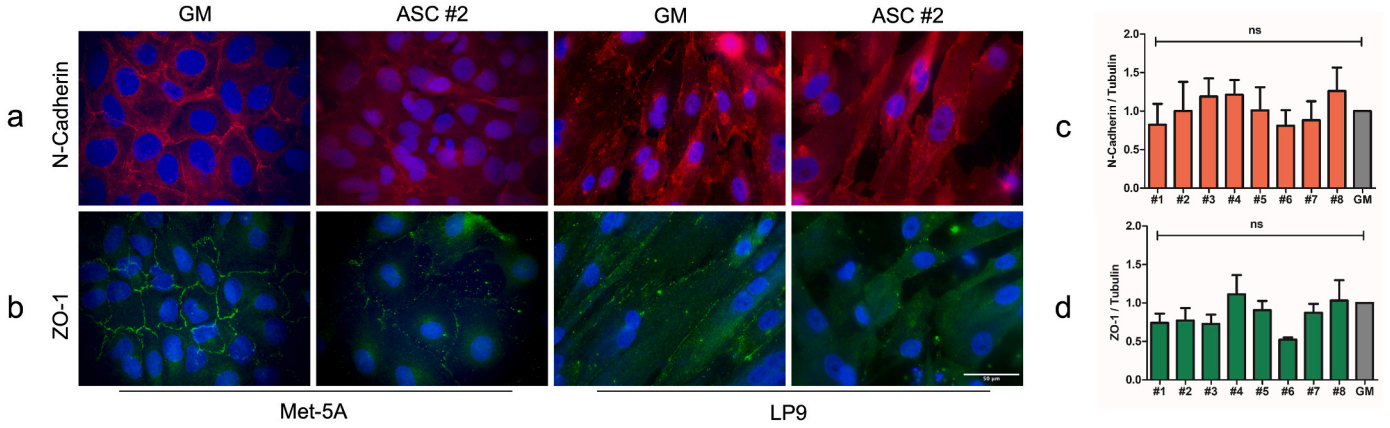


**Fig. 2.** Ascites effects on mesothelium integrity. Immunofluorescent staining of N-Cadherin (a) or ZO-1 (b) expressed by monolayer of Met-5A or LP9 cells after 24 h of incubation with growth medium (GM) or ascites (#2). Cell nuclei were stained with DAPI (blue). Scale bar is 50 μm. Met-5A monolayers were incubated with growth medium (GM) or ascites (#1, #2, #3, #4, #5, #6, #7 and #8) for 24 h to test all ascites samples. Representative western blot for N-Cadherin (c) or ZO-1 (d) expression in Met-5A cells. Equal amounts of total protein (10 μg) were separated on SDS-PAGE under reducing conditions. Tubulin was used as a loading control. Results are given as relative fold change of N-Cadherin or ZO-1 in comparison to tubulin. Data are representative of three independent experiments. *P*-values were calculated by paired one-way ANOVA test with no significant (ns) differences estimated by comparing GM vs ascites.

unchanged and only the organization of actin was disturbed whatever ascites used (Fig. 3b and c). Regarding cells anchoring in growth medium, vinculin-based adhesion structures as indents in staining were localized at the cell membrane shifted to more diffuse intensity and lost their organization in the presence of ascites. In the case of Paxillin staining, a reduction and loss of organization within ascites were observed. Ascites induces disorganization of focal contacts and actin cytoskeletal reorganization, which results in the retraction of the mesothelial cells.

To understand which signaling pathway could be involved in the reorganization of the actin cytoskeleton by ascites, we assayed Rhotekin-RBD and PAK-PBD activation to test the potential involvement of RhoA, Cdc42 and Rac1. Actin immunofluorescence analysis showed an increase in the number of cells rich in membrane ruffles in ascites compared to the growth medium in LP9 cells (Fig. 4a) and Met-5A cells (Fig. 4b). Indeed, ASC#1 and #4 generated more membrane ruffles, but ASC#6 induced a mesenchymal morphology of mesothelial cells. Rac1 activation in ruffle formation has been a firmly established concept in cell biology [32–34]. We found that the staining of Rac1 showed the protein located at the membrane ruffles (Fig. 4a and b). Rhotekin-RBD and PAK-PBD activation was measured on the Met-5A cell monolayers after 30 min or 24 h incubation with growth medium or ascites (#1, #4 or #6). The rate of activation of RhoA and Cdc42 proteins did not significantly change between growth medium and ascites (Supplementary Fig. S2). However, tests showed that the basal activation of Rac1 was low in mesothelial cells, but when these cells were incubated with ascites there was increased activation as early as within 30 min (Fig. 4c). This increase in Rac1 activation in cells had increased by 24 h with ASC#1 and ASC#4. Rac 1 activation in cells with ASC#6 remained constant over time (Fig. 4c).

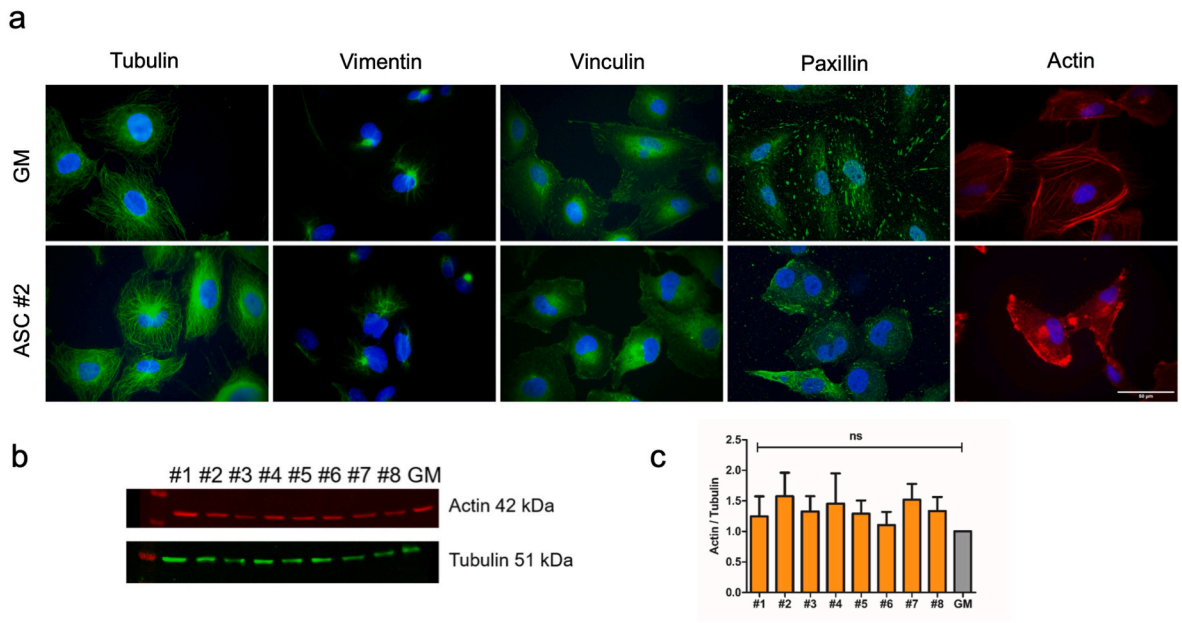


**Fig. 3.** Ascites effects on the cytoskeleton and anchorage of mesothelial cells. (a) Immunofluorescent staining of Tubulin, Vimentin, Actin, Paxillin and Vinculin expressed by Met-5A cells after 24 h of incubation with growth medium (GM) or ascites. Cell nuclei were stained with DAPI (blue). Scale bar is 50 μm. (b) Met-5A monolayers were incubated with growth medium or ascites (#1, #2, #3, #4, #5, #6, #7 and #8) for 24 h to test all ascites samples. Representative western blot for actin expression in Met-5A cells was analyzed. Equal amounts of total protein (10 μg) were separated on SDS-PAGE under reducing conditions. Tubulin was used as a loading control. (c) Relative fold change of actin in comparison to tubulin. Data are representative of three independent experiments. *P*-values were calculated by paired one-way ANOVA test with no significant (ns) differences estimated by comparing GM vs ascites.

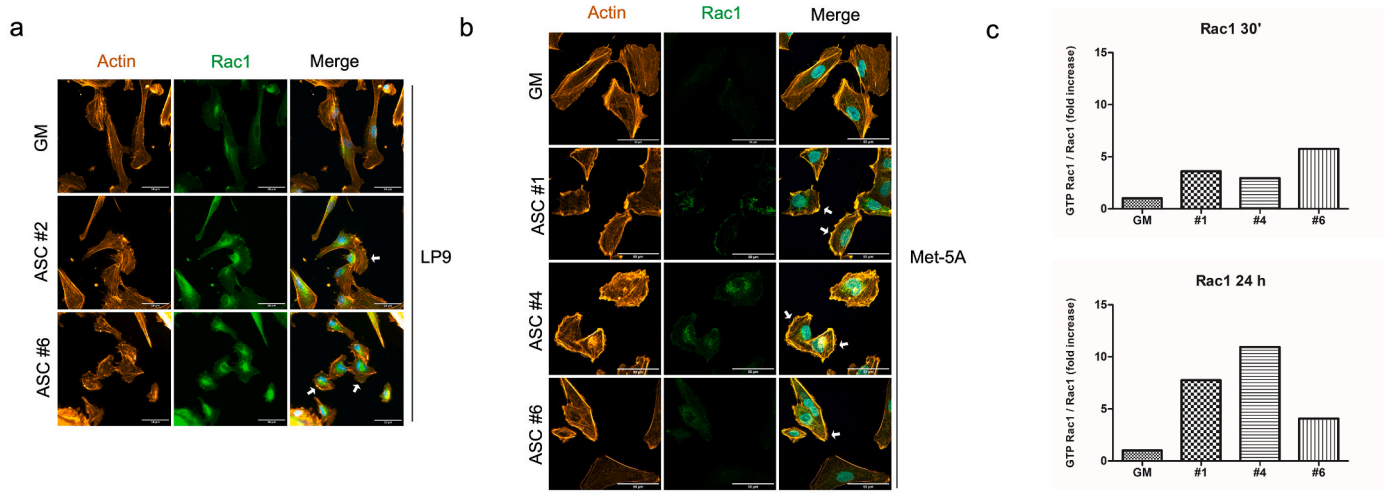


**Fig. 4.** Ascites effect on effector of actin dynamics: Rac1. Mesothelial cells were incubated for 30 min or 24 h with growth medium (GM) or ascites (#1, #2 #4 or #6). Immunofluorescent staining of Rac1 expressed in Met-5A cells (a) or LP9 (b). Cell nuclei were stained with Hoechst (blue). Scale bar is 50 μm. (c) Relative folds of activated Rac1 in comparison to the total protein were given by western blot after Rac1 pull-down activation assay. White arrow shows membrane ruffle. Representative data of three independent experiments.

Ascites causes destabilization of the integrity of mesothelium with a modification of the organization of cell junctions, but without any effect on the synthesis of N-cadherin and ZO-1 by Met-5A cells. Moreover, ascites disorganizes focal contacts and causes actin cytoskeletal reorganization potentially dependent on the activity of Rac1. The latter could be related to the interaction of mesothelial cells with their extracellular microenvironment, in particular ECM proteins.

### 3.3. Ascites contributes to ECM protein organization of mesothelium

Mesothelium is the favorite site of ovarian cancer metastases, the deposit of protein ECM being known to promote the implantation of ovarian cancer cells. To visualize and partially characterize the ECM microenvironment of mesothelium, the localization of ECM protein collagen IV, laminin (basal membrane proteins), fibronectin and fibrinogen (ECM-derived plasmatic/ascitic proteins) were observed in mesothelial cells under classical or ascites conditions by immunofluorescence. Mesothelial cells were seeded in growth medium for 5 days until confluent. The medium was removed and the monolayers incubated in fresh growth medium or ascites for 24 h followed by different staining of ECM proteins. The mesothelial cells stained for collagen IV, laminin and fibronectin in growth medium, but in ascites this expression increased and the staining was more intense, dense and associated with a network organization of proteins (Fig. 5a). Fibrinogen (Fg) and fibrin

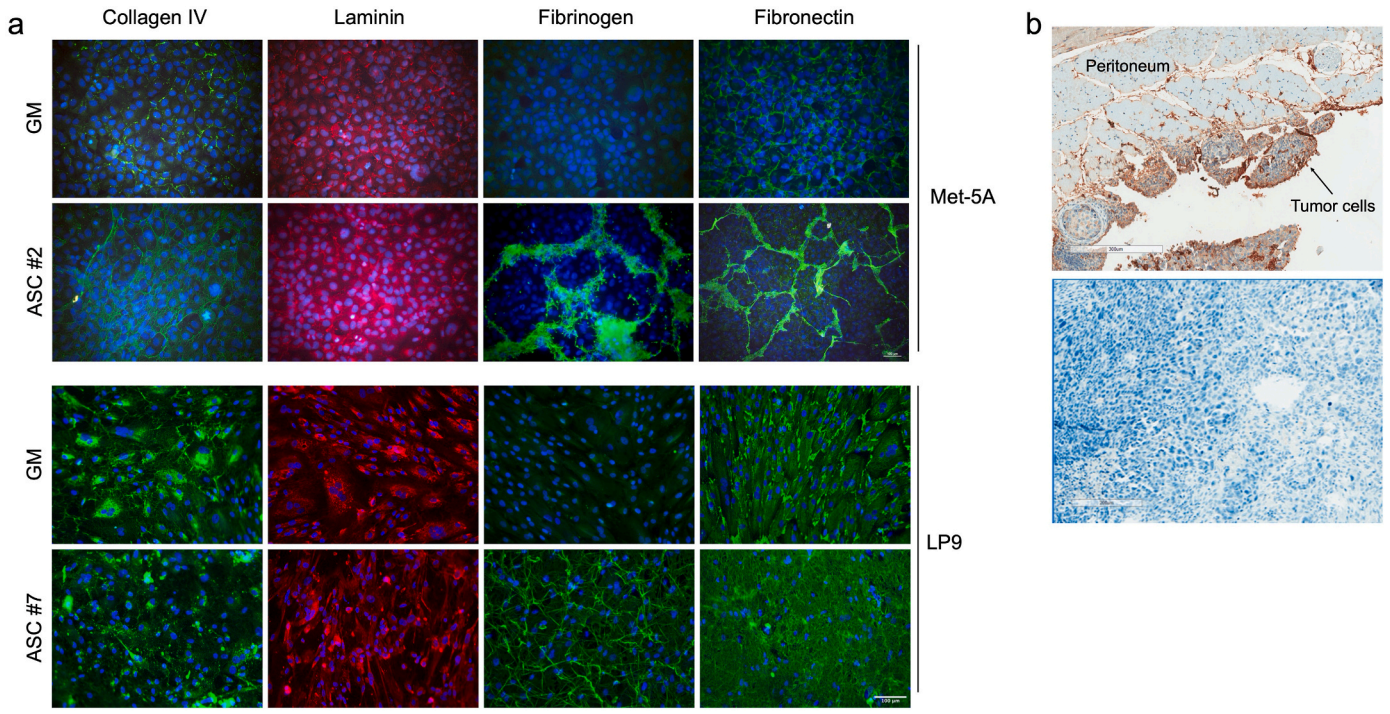


**Fig. 5.** Ascites effects on the expression of matrix proteins of the mesothelial monolayer. (a) Immunofluorescent staining of Collagen IV, Laminin, Fibronectin and Fibrinogen expressed by Met-5A or LP-9 cell monolayer after 24 h of incubation with growth medium (GM) or ascites. Cell nuclei were stained with DAPI (blue). Scale bar is 100 μm. (b) Mesothelium slices of xenograft of ovarian cancer cells injected into the peritoneum of the mouse were subjected to fibrinogen immunolocalization after sacrificing the mouse at 28 days (above). Scale bar is 300 μm. A negative control was performed in the absence of primary antibody (below). Scale bar is 200 μm.

have been identified on peritoneal lining tissues in mice bearing ascites tumors [22,23]. Thus, staining of Fg showed that the mesothelial cells did not express Fg in growth medium; in ascites, staining of Fg, and more specifically fibrin networks in the mesothelial monolayer, was probably due to an intake of fibrinogen and fibrin from the ascites fluid (Fig. 5a). Moreover, *in situ* analysis of the xenograft of ovarian cancer cells injected into the peritoneum of the mouse followed by peroxidase staining confirmed the location of Fg near the mesothelium and around the tumor spheroids adhering to it (Fig. 5b). Thus, ascites allows the densification and reorganization of mesothelium ECM proteins,

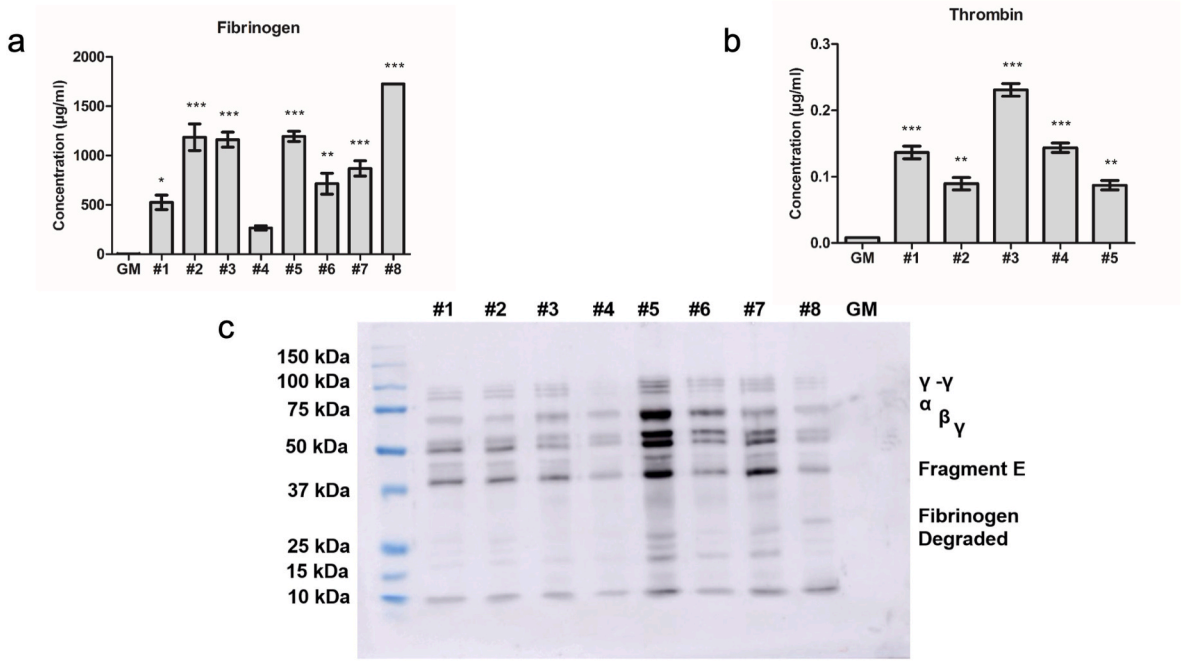


**Fig. 6.** Characterization of fibrinogen, thrombin and fibrin in ascites. Fibrinogen (a) and Thrombin (b) concentrations were quantified by ELISA in ascites and growth medium. Data are representative of three independent experiments and are expressed as mean ± SEM. *P*-values were calculated by paired one-way ANOVA test (*P < 0.05, **P < 0.01, ***P < 0.001) with Growth Medium (GM) vs Ascites (#1, #2, #3, #4, #5, #6, #7, or #8). (c) Representative western blot for Fibrinogen protein expression in ascites or GM. Equal amounts (10 μg) of total ascitic or GM proteins were separated on SDS-PAGE under reducing conditions. MW: Molecular Weight.

especially fibrinogen/fibrin.

### 3.4. Ascites is a reservoir of fibrinogen and fibrin

The presence of Fg and its polymerized form, fibrin, in ascites was investigated. The Fg concentration was determined by the ELISA test in a panel of 8 ascites samples compared with the growth medium. There was heterogeneity of the Fg concentrations according to the range of ascites from to 266 to 1725 μg/ml, the highest concentration approaching that found in the human plasma (2000 to 4000 μg/ml) [35] (Fig. 6a). These fluctuating concentrations reflect the heterogeneity of ascites composition depending on sample source. As expected, growth medium supplemented with 10 % FCS did not contain fibrinogen (Fig. 6a). However, the presence of Fg is insufficient to justify the presence of its polymerized form, fibrin. Thus, thrombin, the main effector of Fg polymerization, was also explored by ELISA assay. Thrombin was present in ascites (#1, #2, #3, #4 and #5) at high concentrations, but significantly lower than for growth medium (Fig. 6b). The presence of Fg was also investigated in the panel of 8 ascites samples (and growth medium) by immunoblotting. As shown in a representative western blot, fibrinogen was detected in all the samples, with different band intensities according to the ascites sample, but not in growth medium. Fg was detected by the presence of 3 bands between 48 and 75 kDa, representative of the 3 pairs of α, β and γ polypeptide chains that constitute the fibrinogen molecule. Moreover, bands of ~85/97 kDa characteristic of γ - γ dimers structures of crosslinked fibrin were present. The proteolysis of fibrin crosslinked by plasmin leads to the DD fragment (D-Dimer consisting of the D domains of 2 fibrin molecules crosslinked by their γ chains) and to the E fragment (central E domain). The bands of E fragment ~40/44 kDa and the degraded fibrinogen have also been detected, which suggests the presence of protagonists of fibrinolysis occurring in ascites (Fig. 6c). These results demonstrate the presence of fibrinogen, thrombin and fibrin in human ascites and show that mechanisms of Fg polymerization and fibrinolysis occur in ovarian cancer ascites.

Figs. 5 and 6 show that the different ascites are the source of fibrinogen and fibrin, which could be reorganized by mesothelial cells. These fibrin networks were analyzed by SEM when the mesothelial monolayers were incubated with growth medium or different ascites (#2, #5 or #6) for 24 h. Our observations confirmed the absence of fibrin networks when mesothelial cells were incubated in growth medium, but heterogenous networks related to the different ascites used, both in terms of quantity and organization, were observed (Fig. 7a). SEM indicated that the networks had well-organized fibers (Fig. 7a, magnification, white arrow). Correlative Light-Electron Microscopy (CLEM) confirmed by Fg staining that the networks correlated to fibrin networks (Fig. 7b). Thus, ascites is a source of Fg and fibrin which deposit on and organize networks in the mesothelium.

Furthermore, ovarian carcinoma dissemination is partly due to spheroids that are released within the peritoneal cavity before implantation into the mesothelium. As shown in Fig. 6, the different ascites were a source of fibrinogen and fibrin that could be reorganized by the ovarian cancer cells. Paraffin sections of spheroids isolated from patient ascites were also analyzed for Fg/fibrin expression. Peroxidase staining confirmed the location of Fg at the periphery and inside spheroids *in situ* (Fig. 8a).

Ascites action of Fg and its polymerized form, fibrin, on tumor spheroid formation was investigated. Ovarian tumor spheroids were generated *in vitro* using the "Hanging Drop" technique (see Materials and Methods) in growth medium or ascites. Their formation was monitored over 5 days. To investigate and visualize the expression and organization of Fg within spheroids, we used immunofluorescence staining on spheroids generated in ascites. Fg was also present and organized in a network with fibrils on the surface of spheroids (Fig. 8b). Expression of Fg showed the protein is provided by ascites because the SKOV3 cells themselves do not express fibrinogen in growth medium (Supplementary Fig. S3). Fluorescent staining showed the specific presence of fibrinogen, but SEM analysis showed a network organization evocative of the organization of the deposition of fibrin, probably brought by ascites, on the surface of the spheroids (Fig. 8c). These results

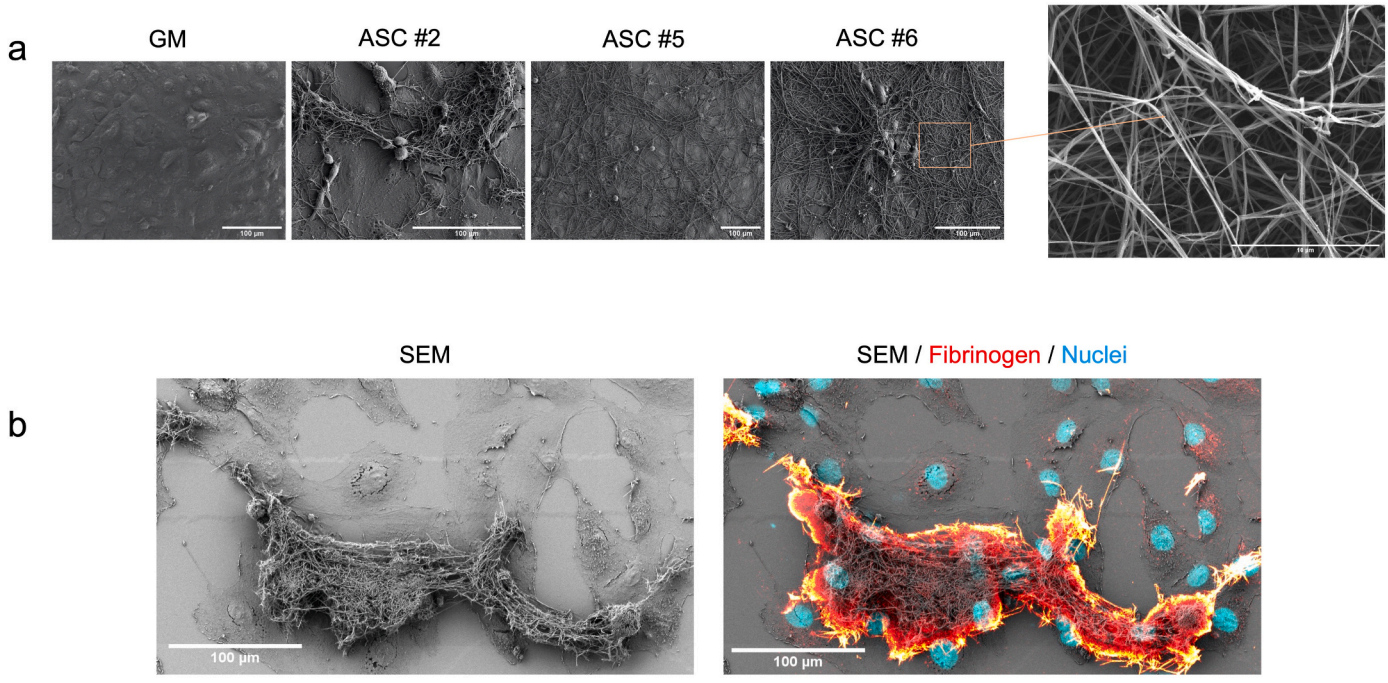


**Fig. 7.** Ascites effects on the organization of fibrin network on the mesothelial monolayer. (a) Met-5A cell monolayer was incubated 24 h with growth medium or different ascites (#2, #5 or #6), and analyzed by SEM. Scale bar is 100 μm. Scale bar of the magnification is 10 μm (white arrow). (b) Mesothelial cell monolayer was incubated 24 h with ascites and was analyzed by Correlative Light-Electron Microscopy (CLEM, right); fibrinogen staining (red) was analyzed using laser scanning confocal microscopy, then the same sample was critical-point dried and analyzed by SEM (left SEM alone, right Merge). Cell nuclei were stained with DAPI (blue). Scale bar is 100 μm.

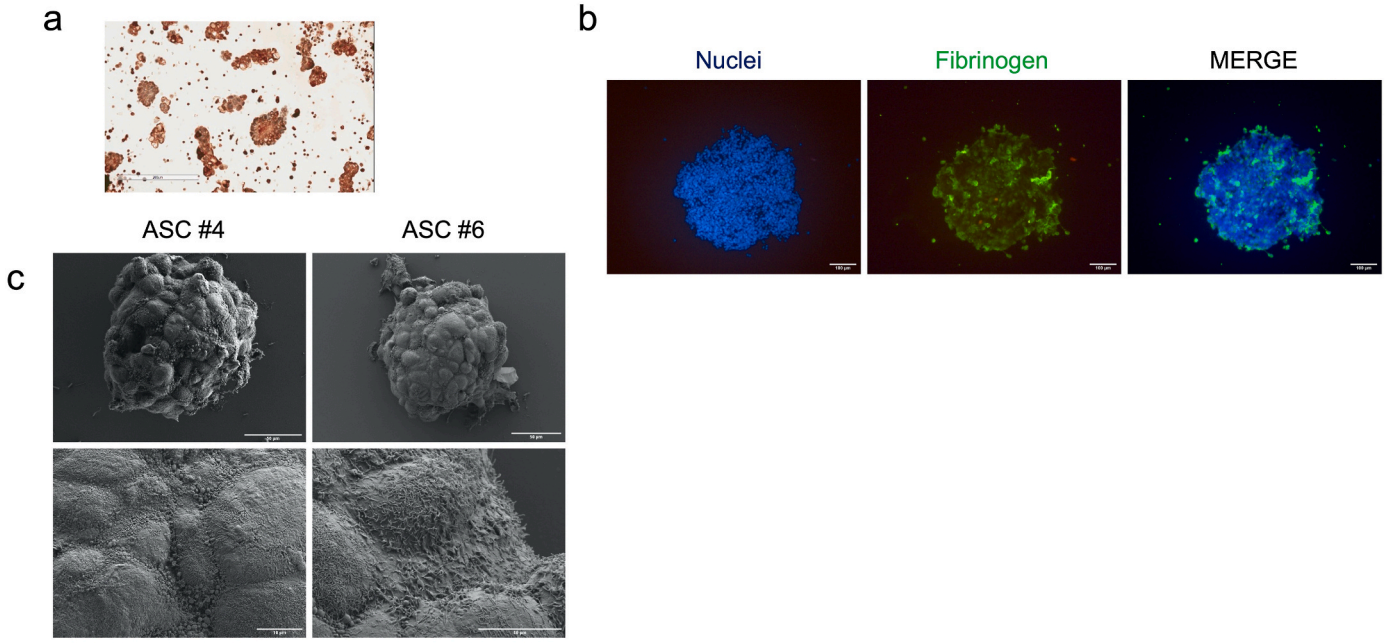


**Fig. 8.** Presence of fibrinogen within ovarian cancer spheroids *in vivo* and *in vitro*. (a) Immunohistochemistry staining of fibrinogen expressed by ovarian cancer spheroids isolated from patient ascites. Scale bar is 200 μm. (b) Immunofluorescent staining of fibrinogen expressed by ovarian cancer spheroids generated *in vitro* in ascites condition (green). Cell nuclei were stained with DAPI (blue). Staining was examined using laser scanning confocal microscopy. Scale bar is 100 μm. (c) Ovarian cancer spheroids were generated *in vitro* in ascites (#4 or #6) and analyzed by Scanning Electron Microscopy (SEM). Scale bars are 50 μm (above) and 10 μm (below).

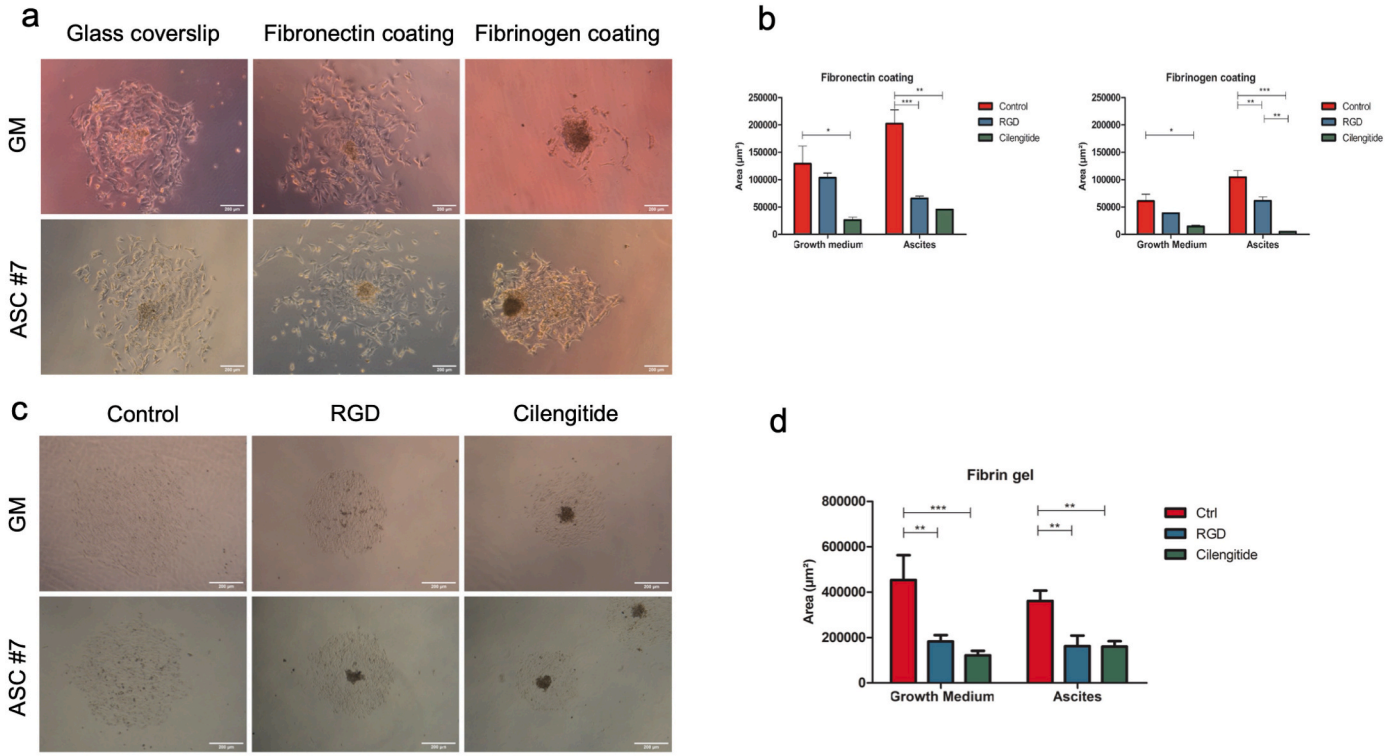


**Fig. 9.** Ascites effects on spheroid dispersion on matrix protein coatings and fibrin gel. (a) Ovarian cancer spheroids were deposited on glass coverslip, fibronectin coating (10 μg/ml) or fibrinogen coating (10 μg/ml) and incubated in growth medium or ascites. Representative light micrographs were taken after 24 h of adhesion. Scale bar is 200 μm. After 24 h of incubation, the areas ($\mu m^2$) of spheroid disaggregation were calculated with the software ImageJ (b). Ovarian cancer spheroids were pre-incubated for 2 h 30 at 4 °C with RGD (100 μg/ml) or Cilengitide (50 μg/ml), before being deposited on the protein coatings (Fibronectin or Fibrinogen) (c) or in a fibrin gel (d) and incubated in growth medium or in ascites. "Control" are spheroids which have been pre-incubated without the blocking peptides (ctrl). Results are representative of at least three independent experiments and are expressed as mean ± SEM. *P*-values were calculated by paired one-way ANOVA test (*P < 0.05, **P < 0.01, ***P < 0.001) with significant differences estimated by comparing control vs RGD or Cilengitide. (c) Representative light micrographs were taken after 24 h of invasion in fibrin gel with RGD or Cilengitide or without peptides (Control). Scale bar is 200 μm.

indicate that ascites is a source of Fg and fibrin surrounding spheroids, which could be involved in their implantation in the mesothelium, favoring metastatic spread.

### 3.5. Ascites promotes integrin-dependent disaggregation of ovarian cancer spheroids and clearance of mesothelial cells

To access the underlying connective tissue of mesothelium and effectively establish metastasis, spheroids were initially implanted into the peritoneal mesothelium ECM matrix. As previously demonstrated, mesothelial cells express Fn, and ascites brought Fg proteins, which deposited and organized fibrin networks on the mesothelium. To study the anchorage of tumor spheroids on the mesothelium, we first explored the ability of spheroids to interact and disaggregate on Fn, Fg and fibrin, i.e. the ability of spheroids to attach to Fn or Fg proteins in ascitic tumor conditions were measured. Spheroids were deposited on glass coverslips (control) or others coated with Fn or Fg, or left in a fibrin gel for 24 h in growth medium or ascites. In growth medium, spheroids adhered to the surfaces, but they disaggregated better on Fn-coated coverslips. Under ascites conditions, spheroids became more disaggregated on all surfaces compared to growth medium (Fig. 9a). Spheroids were able to adhere and disaggregate on different matrix proteins found on the mesothelium and its microenvironment. The disaggregation of spheroids was greater in ascites.

As previously demonstrated, integrins and, more particularly, αv and α5β1 play a key role in the behavior of ovarian cancer cells [36,37]. Thus, spheroids were pre-incubated with the 2 integrin antagonists. The first, the commonly used C(-RGDfc), is a blocking peptide specific to αV integrins, and the second, Cilengitide, is specific to αVβ3, αVβ5 and α5β1 integrins. Following incubation with integrin antagonists, spheroids were deposited on Fn or Fg coating with growth medium or ascites. After 24 h incubation, the surface areas ($\mu m^2$) of Fn or Fg disaggregation were measured. As described above, regarding spheroids without peptides (ctrl), it was confirmed that ascites favored their disaggregation compared to the growth medium on Fn and Fg coatings. In growth medium, the addition of the C(-RGDfc) peptide (RGD) decreased disaggregation on Fn and Fg coatings by 15.7 and 36.6 % respectively. Cilengitide significantly reduced spheroid disaggregation on Fn and Fg coatings by 78.7 and 76.2 % respectively. In ascites, the presence of RGD significantly decreased the ability of spheroids to disaggregate on Fn or Fg by 67.5 and 41.4 % respectively. Whereas cilengitide drastically inhibited spheroid disaggregation on Fn or Fg by 77.4 and 95.3 % respectively (Fig. 9b).

A three-dimensional model in fibrin gel was prepared to observe the disaggregation of spheroids and the invasion of ovarian cancer cells. Spheroids were pre-incubated with the blocking peptides C (-RGDfc) peptide or cilengitide, or without peptides as the control. Spheroids enclosed in fibrin gels were incubated with growth medium or ascites. Those embedded in fibrin gels could disperse under growth medium and ascites conditions after 24 h incubation. However, the blocking peptides seemed to have reduced the disaggregation in fibrin gels (Fig. 9c). At 24 h, the surface areas ($\mu m^2$) of spheroid disaggregation were measured. In growth medium conditions, compared to the control, the addition of RGD or cilengitide significantly inhibited disaggregation and invasion by 59.7 and 73.1 % respectively. In ascites, RGD and cilengitide triggered a similar and significant reduction of invasion by 55 % compared to the control (Fig. 9d).

These results show the "affinity" of tumor spheroids for Fg/fibrin/Fn. The disaggregation of spheroids and the invasion of ovarian cancer cells are dependent on integrin-ECM interactions; in this way, the αV and α5 integrin families seem particularly involved in the disaggregation of spheroids.

To mimic the *in vivo* context, a suitable model of co-culture was developed to assess spheroid cell interaction with the mesothelial monolayer and thus get closer to the pathological conditions of peritoneal implantation. Spheroids were directly allowed to adhere for 6 or 24 h to confluent mesothelial cells in growth medium or ascites. Unlike in growth medium, immunofluorescent staining of the Fg showed that the spheroids were entangled in a Fg network in ascites conditions within 6 h (Fig. 10a and Supplementary Fig. S4a). SEM acquisitions confirmed the presence of fibrin networks around spheroids with the ascites. Fibrin acts as an adhesive matrix which allows the spheroids to adhere to the mesothelium. Cancer cells could leave the spheroids and adhere to the mesothelium (Fig. 10b, black arrow). After 24 h, the spheroids were able to adhere to and disaggregate on the mesothelial monolayer with growth medium or ascites. Under ascites conditions, the spheroids disaggregated faster than in culture medium, and the cells migrated through the mesothelial monolayer (Fig. 10c and Supplementary Fig. S4b). Regardless of the ascites used, spheroid spreading remains similar across various ascites types, with no significant differences observed in spheroid spreading (Supplementary Figure S5, Supplementary Video 1).

Supplementary video related to this article can be found at https://doi.org/10.1016/j.yexcr.2024.114155

The effect of a fibrinogen inhibitor peptide (inh Fg) was assed to further analyze the direct involvement of fibrinogen in the disaggregation of the spheroids. Thus, spheroids were pre-incubated with the inhibitor peptide and were allowed to adhere to the mesothelial monolayer. After 42 h, the spheroids disaggregated more slowly in ascites than in other conditions. Moreover, the inhibitor peptide had no effect on the disaggregation in culture medium (Fig. 11a). Areas of spheroid disaggregation were then measured at different times. A diminution of the areas at 12, 24, 35 and 42 h by 21.5 %, 24.5 %, 29.3 % and 44.7 % respectively was observed in ascites with the inhibitor peptide compared to ascites alone (Fig. 11b).

Transmigration and invasion of ovarian cancer cells through mesothelial cells could be promoted by ascites. Ascites is a component of the peritoneal microenvironment that can act on both cell types, weakening the mesothelium and making cancer cells more invasive, reinforcing mesothelial transmigration and invasion of the underlying tissue. In the co-culture model, tumor spheroids were directly allowed to adhere for 6 h to confluent mesothelial cells in ascites. SEM analysis showed a destabilization of the underlying mesothelial monolayer and the cells seemed to be "pushed" by the spheroid (Fig. 12a, Supplementary Video 2), a phenomenon known as clearance [38]. To analyze this mechanism, the cells of the mesothelial monolayer were stained by incorporating nanoparticles (NPs) before unstained spheroids were placed on it and the co-culture incubated with growth medium or ascites for 24 h. The loss of fluorescence from the monolayer provided proof of mesothelial clearance by the spheroids. Staining of the nuclear DNA with DAPI confirmed that ascites favored the disaggregation of the spheroids (Fig. 12b). Moreover, mesothelial cells stained with NPs showed the absence of fluorescence, and therefore of mesothelial cells, at the location of the spheroid. This suggests that there was a clearance mechanism in addition to the implantation process. Clearance was favored by ascites compared to growth medium (Fig. 12b). An integrin-blocking experiment with their antagonists was carried out to study the involvement of integrins. Spheroids were pre-incubated with the blocking peptides C (-RGDfc) peptide or cilengitide, or without peptides as the control. They were deposited on the NP-staining mesothelial monolayers and incubated with growth medium or ascites. At 24 h, the non-strained areas were measured ($\mu m^2$). In growth medium conditions, compared to the control, addition of RGD or cilengitide significantly inhibited the clearance by 71.3 and 72.6 % respectively. In ascites, RGD triggered a significant reduction of clearance by 64.2 %, whereas cilengitide inhibited more drastically the clearance by 97.1 % (Fig. 12c).

Supplementary video related to this article can be found at https://doi.org/10.1016/j.yexcr.2024.114155

Fibrin in ascites and surrounding ovarian cancer spheroids allows their adhesion to the mesothelium and ascites with its bioactive components promotes their disaggregation, followed by clearance of mesothelial cells. These results show the involvement of the αV and α5β1

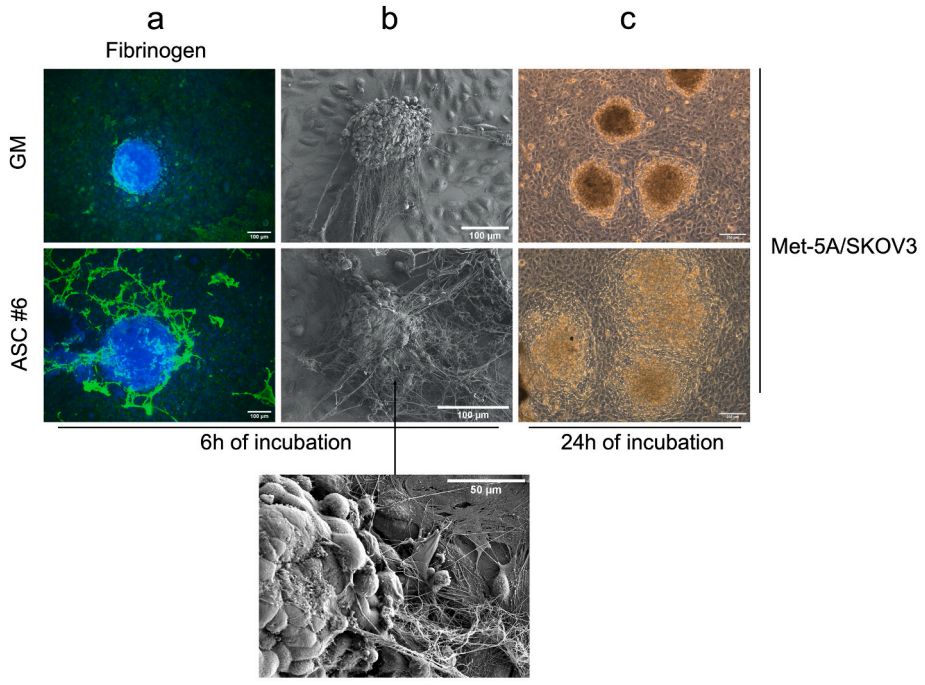


**Fig. 10.** Ascites effects on co-culture model of mesothelial monolayers and spheroids. Ovarian cancer spheroids were deposited on Met-5A monolayer and incubated in growth medium or ascites. (a) After 6 h of incubation, immunofluorescent staining of Fibrinogen (green) and cell nuclei DAPI (blue) was performed. Scale bar is 100 µm. (b) After 6 h of incubation, spheroids were also analyzed by SEM. Scale bar is 100 µm and 50 µm for magnification (black arrow). (c) Representative light micrographs were taken after 24 h of spheroid adhesion. Scale bar is 200 µm.

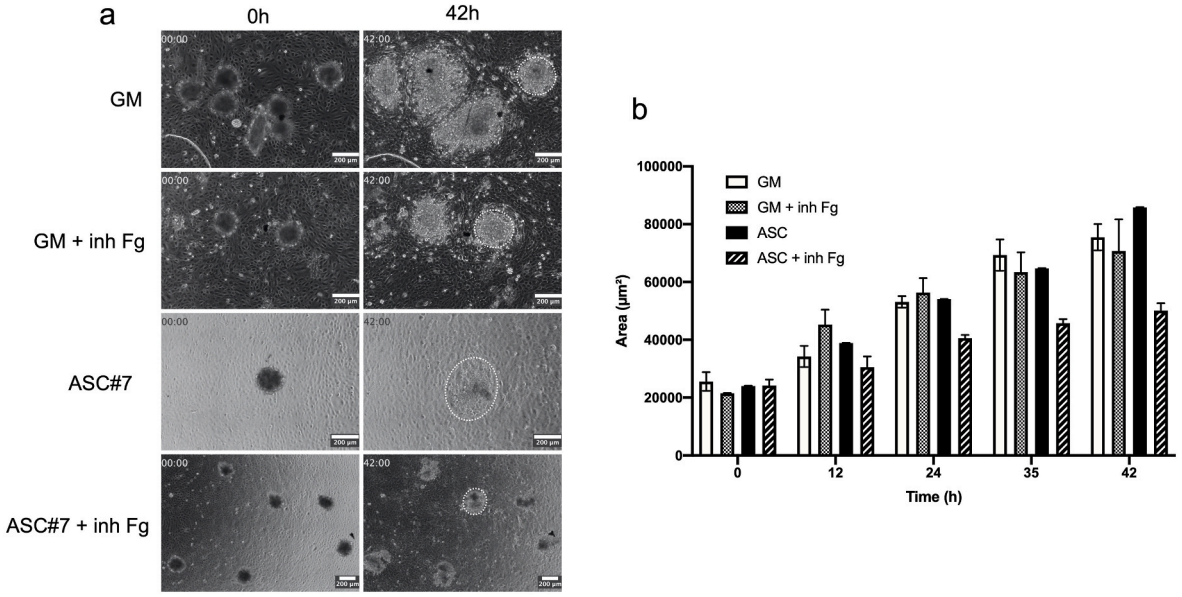


**Fig. 11.** Direct effect of fibrinogen blockage on spheroid dispersion on mesothelial monolayers: (a) Spheroids were pre-incubated for 2 h 30 at 4 °C with the fibrinogen inhibitor peptide (50 µM) before being deposited on mesothelial cell monolayer. The initial photographs (t = 0) were taken 30 min after the spheroids were plated. Photographs were taken every 30 min for a total of 42 h. Scale bar is 200 µm. (b) The areas ($\mu m^2$) of the spheroids were measured (dotted line) with the software ImageJ. Results are representative of at least two independent experiments and are expressed as mean ± SEM.

integrin family in mesothelium clearance by ovarian cancer spheroids.

## 4. Discussion

Ovarian cancer progression is frequently associated with the development of malignant ascites. The shedding of spheroids from the primary tumor found within ascites is thought to promote peritoneal carcinomatosis. We have explored the influence of ascites on ovarian cancer spheroid implantation and dissemination in the peritoneal mesothelium. First, several ascites samples were analyzed and the different results highlighted their heterogeneity. Ascites contains fibrinogen and its activator, thrombin, with some Fg concentrations approaching those found in plasma. The high levels of circulating fibrinogen and the permeability of the vessels lead to an extravasation of fibrinogen into the peritoneal cavity. Plasma fibrinogen levels rise in inflammatory conditions, in the presence of ovarian cancer [19].

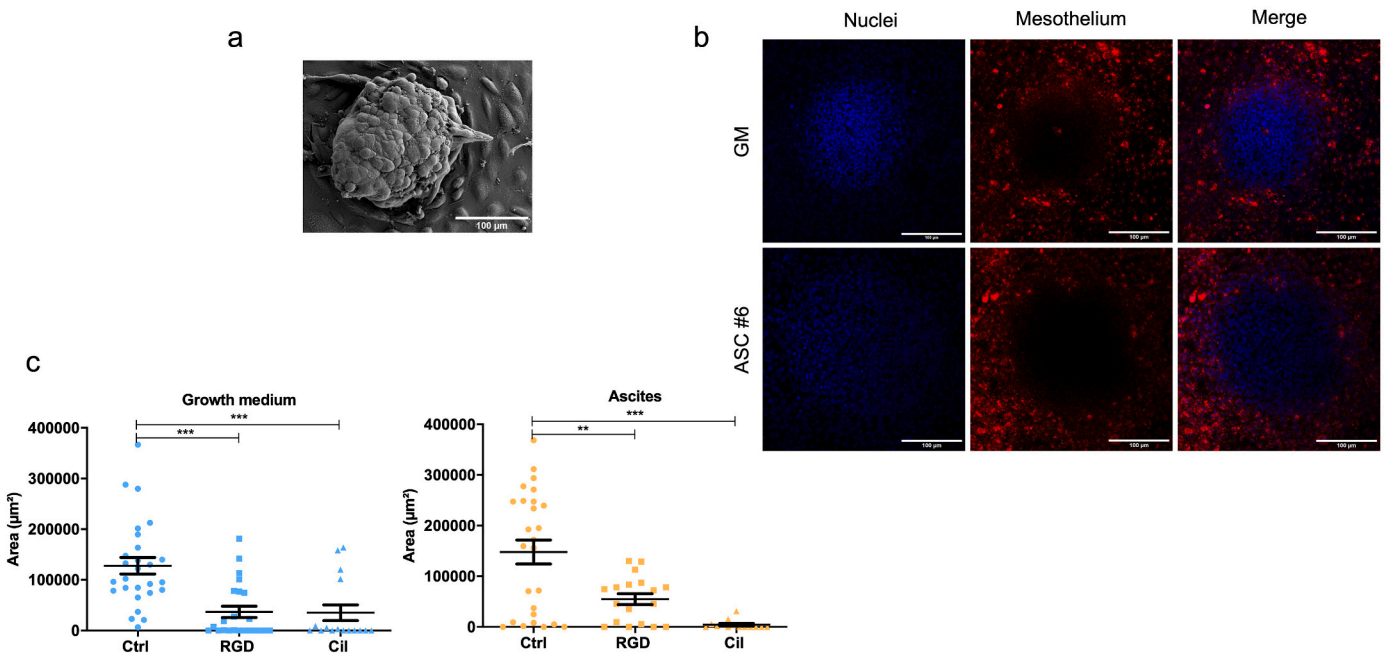


**Fig. 12.** Ascites effects on the clearance of mesothelium by spheroids: (a) Spheroids were deposited on mesothelial monolayer in ascites for 6 h and co-culture was analyzed by SEM. Scale bar is 100 µm. (b) Spheroids were deposited on mesothelial cell monolayer previously stained with nanoparticles (red). Co-cultures were incubated in growth medium or ascites for 24 h. Cell nuclei were stained with DAPI (blue) and co-culture was examined using laser scanning confocal microscopy. The clearance corresponds to the area where there is no nanoparticle fluorescence and consequently the absence of the mesothelial cells. Scale bar is 100 µm. (c) Spheroids were pre-incubated for 2 h 30 at 4 °C with peptides RGD (100 µg/ml) or Cil (50 µg/ml), before being deposited on mesothelial cell monolayer stained with nanoparticles (red). Controls (Ctrl) are spheroids which have been pre-incubated without blocking peptides. Co-cultures were incubated in growth medium or ascites. After 24 h of incubation, the areas ($\mu m^2$) without any nanoparticle staining were measured with the software ImageJ, to quantify the clearance of mesothelial monolayer by spheroids under different conditions. Results are representative of at least three independent experiments and are expressed as mean ± SEM. *P*-values were calculated by paired one-way ANOVA test (**P < 0.01, ***P < 0.001) with significant differences estimated by comparing Ctrl vs RGD or Cilengitide.

Elevated levels of Fg can be explained by an overactivation of the coagulation pathway induced in response to the activation of the immune system to counter the tumor, which results in a pro-coagulant tumor phenotype [21]. When the tumor is in hypoxia, the tissues respond by overexpressing proteins involved in coagulation and fibrinolysis, which promotes the polymerization of Fg into fibrin [39]. We have shown that ascitic fluid contains fibrin. Schneider et al. [10] showed that vitronectin in plasma is a powerful factor promoting cancer cell migration and is chaperoned by fibrinogen [40]. Vitronectin is found in ascites, as it is in plasma. Ascites is also rich in fibrinogen, which suggests an interaction between the 2 proteins, as in plasma.

In mice, the presence of fibrin deposition on the surface of the peritoneal cavity where ovarian cancer cells get trapped has been described [22,23]. After injection of tumor cells, the initial change seen is microvascular hyperpermeability to circulating macromolecules, followed by extravasation of plasma fibrinogen and its coagulation with crosslinked fibrin. Fibrin deposition is harmful in the case of peritoneal dissemination because it traps metastasizing tumor cells. These metastatic deposits become vascularized by the elevation of VEGF-A and IL-8 [22,23–25].

Ascites is a source of Fg and fibrin, which are deposited and organized in networks on the mesothelium. Fg and fibrin are key elements in the creation of a suitable microenvironment for ovarian cancers and play a key role in the development of metastatic niches.

We also set out to follow its impact on the privileged site of metastasis, the mesothelium, and on spheroid formation. Disturbances occur in the mesothelial cell cycle and/or cell death due to ascites. Ascites alters the homeostasis of the mesothelium, probably favoring the anchorage and metastasis of cancer cells. Ascites destabilizes the mesothelial monolayer by modifying ZO-1 and N-cadherin junctions. The change in the organization of these cell junction proteins may be a consequence of the rearrangement of the actin cytoskeleton following the modification in the expression of the Rac1 pathway [41,42]. Mesothelial cells exposed to malignant ascites from type I tumors (clear and endometrioid cells) do not change their expression of E-cadherin (adherent junctions), occludin (tight junctions) and desmoglein (desmosome), but have decreased expression of Connexin 43 (GAP junctions). On the other hand, the mesothelial cells subjected to a type II malignant ascites (serous and undifferentiated) are characterized by a significant reduction in the expression of the intercellular junctions tested [43]. We also show disorganization of focal contacts and actin cytoskeletal reorganization by ascites, which result in a retraction of the mesothelial cells. This retraction could be partly due to cellular signaling engaged by the several molecules contained in ascites. Within ascites, tumor cells, mesothelial-derived CAFs, and infiltrating leukocytes produce a multitude of factors, including but not limited to cytokines, chemokines, and growth factors. These autocrine and paracrine soluble molecules form complex signaling networks that govern, in part, tumor-peritoneum interactions. Thus, cytokines, chemokines, growth factors, miRNAs, MMP and also proteins contained in exosomes may contribute to this cell retraction and could participate in destabilizing cellular anchors [44]. TGFb1, for example, seems to be a good candidate for stimulating this event [45]. Moreover, ascites enhances the modification and densification of the ECM network on mesothelium, which illustrates the remodeling of the mesothelial microenvironment suitable for tumor cell implantation.

Moreover, the properties of senescent cells favor cancer progression. Ksiazek et al. [46] have demonstrated the presence of senescent human peritoneal mesothelial cells near cancerous tissue, which could allow the formation of a metastatic niche that facilitates the intraperitoneal growth of malignant tumors. In this senescence process, ascites plays an important role, as there is an increase in senescence in mesothelial cells exposed to malignant ascites [47,48]. To summarize, our results on the destabilization of cell-cell and cell-ECM interactions disturbed the

mesothelial monolayer, making it fragile and facilitating the implantation of cancer cells.

To mimic three-dimensional free-floating ovarian cancer spheroids, the hanging-drop technique was used. This approach demonstrated that ascites improves the capacity of ovarian cancer cells to form spheroids when they are maintained in a culture state independent of anchoring. The use of another culture model previously established to generate spheroids in non-adherent conditions, i.e. when the culture flasks were covered with agarose, showed similar results in the formation and compaction of spheroids between ascites and growth medium [12]. However, the spheroids were of different sizes, heterogeneous shapes and different states of compaction, which did not allow them to be used for reproducible experiments. The hanging-drop technique ensured seeding at a homogeneous cell density, which allows reproducible results. Our spheroids were generated with the SKOV3 cell line; however, we also produced spheroids with the IGROV1 cell line but they were much less compact. The formation of compact spheroids is stronger when comprised of ovarian cell lines that already had a mesenchymal phenotype [49]. Indeed, the exposure of ovarian cancer cell lines to ascites leads to changes in cellular morphologies. Within ascites, IGROV1 cells harbor an epithelial phenotype, whereas SKOV3 cells, initially harbor an intermediate mesenchymal phenotype, strengthen their mesenchymal markers [50]. Mesenchymal cell lines also have a higher migratory and invasive capacity than those cell lines which did not form compact spheroids; indeed, the SKOV3 line is more invasive than the IGROV1 line [49,50]. Matte et al. [51] found mesothelial cells at the center of the spheroids (*in vivo* and *in vitro* with the hanging-drop technique), which makes the spheroids more compact. Ascites promotes the compaction of spheroids but is also a source of flaking mesothelial cells that become incorporated into the spheroids and also promote compaction. In these "hybrid" spheroids there is a strong expression of β1 integrins, which would promote attachment to the mesothelium. The three-dimensional organization of compact spheroids leads to poor delivery of the chemotherapeutic agents to the inner regions of the spheroids and subsequently chemoresistance [49].

Characterization of spheroids by fluorescent analysis detects the presence of fibrinogen. In a previous study [12] we showed the role of Vn and their integrin receptors in the initial formation of spheroids. Under ascites conditions the spheroids express and aggregate various matrix proteins on their surface, and these might be involved in their implantation in the mesothelium, which would favor metastasis.

Moreover, characterization of the mesothelial extracellular matrix proteins by immunofluorescent staining showed the presence of fibronectin, laminin, vitronectin and fibrinogen, and their remodeling on networks in ascites. The disaggregation of spheroids on different coatings of fibronectin and fibrinogen (proteins present on the mesothelium) has shown that ascites promotes this disaggregation. Blockade of integrins by the RGD peptide and cilengitide, or of fibrinogen by the inhibitor peptide reduced the disaggregation of the spheroids on the different matrices. Kenny et al. [52] have shown that the blocking of the production of fibronectin in mesothelial cells leads to decreased adhesion, invasion, proliferation and metastasis of single ovarian cancer cells. The authors also showed that inhibition of the interaction of integrins α5 and β1 with fibronectin blocks the initial and late stages of metastases. *In vitro,* spheroids were, like our results, completely disaggregated on type I collagen substrates. In addition, a monoclonal antibody against the β1 integrin subunit significantly inhibited spheroid disaggregation on all of the proteins tested (laminin, fibronectin, collagen IV) [53]. Spheroids isolated from patient ascites completely disaggregated on the components of the extracellular matrix (laminin, fibronectin, collage I, collagen IV and hyaluronan) [3]. Spheroid adhesion to hyaluronic acid expressed by mesothelial cells can be directed by CD44 expressed on the surface of spheroids derived from patients [17]. The absence of CD44 expression can decrease spheroid formation [54].

These results, which are in agreement with ours, prove the importance of ECM proteins expressed on the surface of mesothelium or by spheroids during the different stages of ovarian cancer metastasis, and the involvement of integrins in these mechanisms.

*In vitro,* we showed that ascites promotes the dispersion of spheroids on the mesothelial monolayer. After implantation *in vivo*, the spheroids could "push aside" mesothelial cells and pass through it (transmesothelial migration) to access the underlying tissues and form metastases [55]. Iwanicki et al. [38] have shown that blocking the expression of talin I in cancerous spheroids inhibits the clearance of mesothelial cells. In addition, the recruitment of talin I seems necessary for the clearance of mesothelial cells generated by myosin. Blocking the α5β1 integrin in ovarian cancer cells decreases mesothelial cell clearance, whereas overexpression of the α5β1 integrin increases their clearance. Together, these data show that ovarian cancer spheroids "push aside" mesothelial cells dependent on α5β1 integrins and talin. Our results corroborate the involvement of the α5β1 and show the involvement of the αV integrin family in mesothelium clearance by ovarian cancer cell spheroids. Cilengitide is a cyclic RGD pentapeptide used in the treatment of glioblastomas and is being studied for treatment of several other tumors. This drug is the first small anti-angiogenic molecule targeting integrins αvβ3, αvβ5 and α5β1. With ascites, cilengitide has a better efficacy, which can be explained in ascites by the focal contacts being destabilized; it may be a redeployment of these integrins which makes them more accessible to cilengitide under these conditions.

The use of a 3D model is essential in the study of ovarian cancer, especially cancer metastasis processes *in vitro*. The co-culture model developed between healthy mesothelial monolayer cells and ovarian cancer spheroids allowed us to follow the effects of ascites on the disaggregation of spheroids on the mesothelium and the clearance of the mesothelial monolayer. This 3D co-culture model mimics the early stages of peritoneal implantation and comes closer to *in vivo* conditions. In ovarian cancer, a high level of chemoresistance occurs and a difference in sensitivity to treatments between cells in 2D and 3D models has been demonstrated. It is therefore necessary to test drugs on cancer cells when they are in a 3D model that mimics the *in vivo* context [56,57]. In addition, the composition of the matrix of this model plays a role both in the composition and the quantity of the matrix elements. Our results, which show different responses to the presence of fibrinogen and fibrin in ascites, neighboring the mesothelium and around the spheroids, indicate the importance of this protagonist. Moreover, cancer cells can invade fibrin gels. Fibrin serves as a temporary matrix to facilitate neovascularization and the proliferation of fibroblasts [58]. This is why it is important to include this protagonist in the 3-dimensional modeling of co-cultures. The importance of models simulating the *in vivo* context is the use of the most cellular and acellular protagonists found in the microenvironment. *In vitro* 3D models can screen different drugs and measure their effects on cancer and healthy cells. In addition, the model can be made more complex by adding subsequent conjunctive cells, such as fibroblasts or even adipocytes; indeed, several studies show the involvement of these non-cancer cells in the metastasis of ovarian cancer [59–62].

## 5. Conclusion

In conclusion, ascites, which is a unique microenvironment, affects the integrity of the mesothelium and promotes the integrin-dependent implantation and dispersion of OC spheroids in the mesothelium. The ascites fibrinogen/fibrin composition promotes the creation of a pre-metastatic niche for ovarian cancer metastases and the formation of secondary malignant tumor. Understanding the impacts of ascites is essential to better understanding the evolution of ovarian cancer.

## Ethics approval and consent to participate

The ascites samples were collected at the F. Baclesse Cancer Center (Caen, France), were certified cytologically as positive for malignant

cells and stored in the OvaRessources Biological Resources Center (BRC) (NF–S 96900 quality management, AFNOR N°2016:72860.5). The medical officer and the scientific officer of the BRC are respectively Dr Cécile Blanc Fournier and Dr Laurent Poulain. All biological collection from BRC was declared by the Project Manager of the Clinical Research Department (Alexandra Leconte) to the French Ministry of Education, Health and Research (MESR) (N°DC-2010-1243 and amendments DC-2013-1849, DC-2016-2641 and DC-2017-2923). The collection of samples was approved on 17 September 2011. We obtained written informed consent from the patients. The study was approved by the CPP North West III ethical committee (Committee for the Protection of Persons).

## Consent for publication

All authors have read and approved the manuscript and give consent for publication.

## Availability of data and materials

All data supporting the findings of this study are available within the paper and its supplementary information files.

## Funding

This work was supported by the Ligue Contre le Cancer, Comité du Val d'Oise, France.

## CRediT authorship contribution statement

**Carine Laurent-Issartel:** Writing – review & editing, Writing – original draft, Visualization, Validation, Resources, Methodology, Investigation, Formal analysis, Data curation. **Alexandra Landras:** Writing – review & editing, Visualization, Validation, Resources, Methodology, Investigation, Formal analysis, Data curation. **Rémy Agniel:** Visualization, Validation, Software, Resources, Methodology, Formal analysis. **Florence Giffard:** Resources, Methodology. **Cécile Blanc-Fournier:** Resources, Methodology. **Elisabete Da Silva Cruz:** Methodology, Formal analysis. **Chahrazed Habes:** Methodology, Investigation, Formal analysis. **Johanne Leroy-Dudal:** Writing – review & editing. **Franck Carreiras:** Writing – review & editing, Writing – original draft, Validation, Supervision, Resources, Project administration, Methodology, Funding acquisition, Data curation, Conceptualization. **Sabrina Kellouche:** Writing – review & editing, Writing – original draft, Validation, Supervision, Resources, Project administration, Methodology, Funding acquisition, Data curation, Conceptualization.

## Declaration of competing interest

The authors declare that they have no known competing financial interests or personal relationships that could have appeared to influence the work reported in this paper.

## Data availability

All data supporting the findings of this study are available within the paper and its supplementary information files.

## Acknowledgments

The authors thank MecuP group members for constructive discussions. The authors thank Dr. Andreas Reich from Laboratoire de Bioimagerie et Pathologies (UMR CNRS 7021) for providing us with his nanoparticles. The authors thank M. Briand from the François Baclesse Comprehensive Cancer Center and the Center de Ressource Biologique for their support in obtaining ascites samples used in this study. This study was conducted using the facilities of the Plateforme Microscopies & Analyses, Federation I-Mat (FR4122) of CY Cergy Paris University (France). The manuscript was proofread by a professional translator and editor.

## Appendix A. Supplementary data

Supplementary data to this article can be found online at https://doi.org/10.1016/j.yexcr.2024.114155.

## Abbreviations

| | |
|---|---|
| 3D | Three-dimensional |
| ASC | Ascites |
| BSA | BiCinchoninic Acid Assay |
| CLEM | Correlative Light-Electron Microscopy |
| Ctrl | Control |
| ECM | extracellular matrix |
| EGF | epidermal growth factor |
| FBS | fetal bovine serum |
| Fg | fibrinogen |
| Fn | fibronectin |
| GM | growth medium |
| inh Fg | Inhibitor Fg |
| NPs | nanoparticles |
| OC | ovarian cancer |
| PAK-PBD | p21 Activated Kinase I - p21Binding Domain |
| PFA | paraformaldehyde |
| rhotekin-RBD | rhotekin - Rho Binding Domain |
| RT | room temperature |
| SEM | Standard Error of the Mean |

## References

[1] E. Kipps, D.S.P. Tan, S.B. Kaye, Meeting the challenge of ascites in ovarian cancer: new avenues for therapy and research, Nat. Rev. Cancer 13 (2013) 273–282, https://doi.org/10.1038/nrc3432.

[2] L. Heyman, S. Kellouche, J. Fernandes, S. Dutoit, L. Poulain, F. Carreiras, Vitronectin and its receptors partly mediate adhesion of ovarian cancer cells to peritoneal mesothelium in vitro, Tumour Biol. J. Int. Soc. Oncodevelopmental Biol. Med. 29 (2008) 231–244, https://doi.org/10.1159/000152941.

[3] K.M. Burleson, M.P. Boente, S.E. Pambuccian, A.P.N. Skubitz, Disaggregation and invasion of ovarian carcinoma ascites spheroids, J. Transl. Med. 4 (2006) 6, https://doi.org/10.1186/1479-5876-4-6.

[4] K. Shield, M.L. Ackland, N. Ahmed, G.E. Rice, Multicellular spheroids in ovarian cancer metastases: biology and pathology, Gynecol. Oncol. 113 (2009) 143–148, https://doi.org/10.1016/j.ygyno.2008.11.032.

[5] H.A. Kenny, S. Kaur, L.M. Coussens, E. Lengyel, The initial steps of ovarian cancer cell metastasis are mediated by MMP-2 cleavage of vitronectin and fibronectin, J. Clin. Invest. 118 (2008) 1367–1379, https://doi.org/10.1172/JCI33775.

[6] A. Ayhan, M. Gultekin, C. Taskiran, P. Dursun, P. Firat, G. Bozdag, N.Y. Celik, K. Yuce, Ascites and epithelial ovarian cancers: a reappraisal with respect to different aspects, Int. J. Gynecol. Cancer Off. J. Int. Gynecol. Cancer Soc. 17 (2007) 68–75, https://doi.org/10.1111/j.1525-1438.2006.00777.x.

[7] D.S.P. Tan, R. Agarwal, S.B. Kaye, Mechanisms of transcoelomic metastasis in ovarian cancer, Lancet Oncol. 7 (2006) 925–934, https://doi.org/10.1016/S1470-2045(06)70939-1.

[8] M.-L. Puiffe, C. Le Page, A. Filali-Mouhim, M. Zietarska, V. Ouellet, P.N. Tonin, M. Chevrette, D.M. Provencher, A.-M. Mes-Masson, Characterization of ovarian cancer ascites on cell invasion, proliferation, spheroid formation, gene expression in an in vitro model of epithelial ovarian cancer, Neoplasia 9 (2007) 820, https://doi.org/10.1593/neo.07472. IN8.

[9] D. Lane, N. Goncharenko-Khaider, C. Rancourt, A. Piché, Ovarian cancer ascites protects from TRAIL-induced cell death through αvβ5 integrin-mediated focal adhesion kinase and Akt activation, Oncogene 29 (2010) 3519–3531, https://doi.org/10.1038/onc.2010.107.

[10] L. Carduner, R. Agniel, S. Kellouche, C.R. Picot, C. Blanc-Fournier, J. Leroy-Dudal, F. Carreiras, Ovarian cancer ascites-derived vitronectin and fibronectin: combined purification, molecular features and effects on cell response, Biochim. Biophys. Acta 1830 (2013) 4885–4897, https://doi.org/10.1016/j.bbagen.2013.06.023.

[11] L. Gong, Y. Zheng, S. Liu, Z. Peng, Fibronectin regulates the dynamic formation of ovarian cancer multicellular aggregates and the expression of integrin receptors, Asian Pac. J. Cancer Prev. APJCP (2018), https://doi.org/10.22034/APJCP.2018.19.9.2493.

[12] S. Kellouche, J. Fernandes, J. Leroy-Dudal, O. Gallet, S. Dutoit, L. Poulain, F. Carreiras, Initial formation of IGROV1 ovarian cancer multicellular aggregates

involves vitronectin, Tumor Biol. 31 (2010) 129–139, https://doi.org/10.1007/s13277-010-0017-9.
[13] L. Carduner, C.R. Picot, J. Leroy-Dudal, L. Blay, S. Kellouche, F. Carreiras, Cell cycle arrest or survival signaling through αv integrins, activation of PKC and ERK1/2 lead to anoikis resistance of ovarian cancer spheroids, Exp. Cell Res. 320 (2014) 329–342, https://doi.org/10.1016/j.yexcr.2013.11.011.
[14] A. Frankel, R. Buckman, R.S. Kerbel, Abrogation of taxol-induced G2-M arrest and apoptosis in human ovarian cancer cells grown as multicellular tumor spheroids, Cancer Res. 57 (1997) 2388–2393.
[15] E. Lengyel, Ovarian cancer development and metastasis, Am. J. Pathol. 177 (2010) 1053–1064, https://doi.org/10.2353/ajpath.2010.100105.
[16] J. Ren, Y. Xiao, L.S. Singh, X. Zhao, Z. Zhao, L. Feng, T.M. Rose, G.D. Prestwich, Y. Xu, Lysophosphatidic acid is constitutively produced by human peritoneal mesothelial cells and enhances adhesion, migration, and invasion of ovarian cancer cells, Cancer Res. 66 (2006) 3006–3014, https://doi.org/10.1158/0008-5472.CAN-05-1292.
[17] S.A. Cannistra, G.S. Kansas, J. Niloff, B. DeFranzo, Y. Kim, C. Ottensmeier, Binding of ovarian cancer cells to peritoneal mesothelium in vitro is partly mediated by CD44H, Cancer Res. 53 (1993) 3830–3838.
[18] T. Strobel, L. Swanson, S.A. Cannistra, In vivo inhibition of CD44 limits intra-abdominal spread of a human ovarian cancer xenograft in nude mice: a novel role for CD44 in the process of peritoneal implantation, Cancer Res. 57 (1997) 1228–1232.
[19] Y. Luo, H.S. Kim, M. Kim, M. Lee, Y.S. Song, Elevated plasma fibrinogen levels and prognosis of epithelial ovarian cancer: a cohort study and meta-analysis, J. Gynecol. Oncol. 28 (2017), https://doi.org/10.3802/jgo.2017.28.e36.
[20] G.-F. von Tempelhoff, L. Heilmann, G. Hommel, Correspondence re, N.C. Denko, A. J. Giaccia, Tumor hypoxia, the physiological link between trousseau's syndrome (Carcinoma-induced coagulopathy) and metastasis, Cancer Res. 61 (2001) 795–798. Cancer Res. 61 (2001) 7697–7698.
[21] G.J. Caine, P.S. Stonelake, G.Y.H. Lip, S.T. Kehoe, The hypercoagulable state of malignancy: pathogenesis and current debate, Neoplasia N. Y. N 4 (2002) 465–473, https://doi.org/10.1038/sj.neo.7900263.
[22] J.A. Nagy, M.S. Meyers, E.M. Masse, K.T. Herzberg, H.F. Dvorak, Pathogenesis of ascites tumor growth: fibrinogen influx and fibrin accumulation in tissues lining the peritoneal cavity, Cancer Res. 55 (1995) 369–375.
[23] J.A. Nagy, E.M. Masse, K.T. Herzberg, M.S. Meyers, K.T. Yeo, T.K. Yeo, T. M. Sioussat, H.F. Dvorak, Pathogenesis of ascites tumor growth: vascular permeability factor, vascular hyperpermeability, and ascites fluid accumulation, Cancer Res. 55 (1995) 360–368.
[24] E. Pretorius, W.A. Vieira, H.M. Oberholzer, R.E.J. Auer, Comparative scanning Electron microscopy of platelets and fibrin networks of human and differents animals, Int. J. Morphol. 27 (2009) 69–76, https://doi.org/10.4067/S0717-95022009000100013.
[25] S. Shahid, A. Iman, U. Matti, K. Rachid, A. Assaf, C. Eveno, P. Marc, M. Massoud, Fibrin deposit on the peritoneal surface serves as a niche for cancer expansion in carcinomatosis patients, Neoplasia N. Y. N 21 (2019) 1091–1101, https://doi.org/10.1016/j.neo.2019.08.006.
[26] L. Poulouin, O. Gallet, M. Rouahi, J.M. Imhoff, Plasma fibronectin: three steps to purification and stability, Protein Expr. Purif. 17 (1999) 146–152, https://doi.org/10.1006/prep.1999.1103.
[27] R. Foty, A simple hanging drop cell culture protocol for generation of 3D spheroids, J. Vis. Exp. (2011), https://doi.org/10.3791/2720.
[28] M.-H. Louis, S. Dutoit, Y. Denoux, P. Erbacher, E. Deslandes, J.-P. Behr, P. Gauduchon, L. Poulain, Intraperitoneal linear polyethylenimine (L-PEI)-mediated gene delivery to ovarian carcinoma nodes in mice, Cancer Gene Ther. 13 (2006) 367–374, https://doi.org/10.1038/sj.cgt.7700893.
[29] P. Paul-Gilloteaux, X. Heiligenstein, M. Belle, M.-C. Domart, B. Larijani, L. Collinson, G. Raposo, J. Salamero, eC-CLEM: flexible multidimensional registration software for correlative microscopies, Nat. Methods 14 (2017) 102–103, https://doi.org/10.1038/nmeth.4170.
[30] B. Andreiuk, A. Reisch, M. Lindecker, G. Follain, N. Peyriéras, J.G. Goetz, A. S. Klymchenko, Fluorescent polymer nanoparticles for cell barcoding in vitro and in vivo, Small Weinh. Bergstr. Ger. 13 (2017), https://doi.org/10.1002/smll.201701582.
[31] K. Suehiro, J.W. Smith, E.F. Plow, The ligand recognition specificity of beta 3 integrins, J. Biol. Chem. 271 (1996) 10365–10371, https://doi.org/10.1074/jbc.271.17.10365.
[32] P. Aspenström, Å. Fransson, J. Saras, Rho GTPases have diverse effects on the organization of the actin filament system, Biochem. J. 377 (2004) 327–337, https://doi.org/10.1042/bj20031041.
[33] E.S. Chhabra, H.N. Higgs, The many faces of actin: matching assembly factors with cellular structures, Nat. Cell Biol. 9 (2007) 1110–1121, https://doi.org/10.1038/ncb1007-1110.
[34] S.J. Heasman, A.J. Ridley, Mammalian Rho GTPases: new insights into their functions from in vivo studies, Nat. Rev. Mol. Cell Biol. 9 (2008) 690–701, https://doi.org/10.1038/nrm2476.
[35] M.W. Oswald, H.H. Hunt, J. Lazarchick, Normal range of plasma fibrinogen, Am. J. Med. Technol. 49 (1983) 57–59.
[36] J.S. Desgrosellier, D.A. Cheresh, Integrins in cancer: biological implications and therapeutic opportunities, Nat. Rev. Cancer 10 (2010) 9–22, https://doi.org/10.1038/nrc2748.
[37] M. Kobayashi, K. Sawada, T. Kimura, Potential of integrin inhibitors for treating ovarian cancer: a literature review, Cancers 9 (2017), https://doi.org/10.3390/cancers9070083.
[38] M.P. Iwanicki, R.A. Davidowitz, M.R. Ng, A. Besser, T. Muranen, M. Merritt, G. Danuser, T. Ince, J.S. Brugge, Ovarian cancer spheroids use myosin-generated force to clear the mesothelium, Cancer Discov. 1 (2011) 144–157, https://doi.org/10.1158/2159-8274.CD-11-0010.
[39] N.C. Denko, A.J. Giaccia, Tumor Hypoxia, the Physiological Link between Trousseau's Syndrome (Carcinoma-induced Coagulopathy) and Metastasis, Cancer Res. 61 (3) (2001) 795–798. https://cancerres.aacrjournals.org/content/61/3/795 (accessed August 14, 2019).
[40] G. Schneider, E. Bryndza, A. Poniewierska-Baran, K. Serwin, M. Suszynska, Z. P. Sellers, M.L. Merchant, A. Kaliappan, J. Ratajczak, M. Kucia, N.C. Garbett, M. Z. Ratajczak, Evidence that vitronectin is a potent migration-enhancing factor for cancer cells chaperoned by fibrinogen: a novel view of the metastasis of cancer cells to low-fibrinogen lymphatics and body cavities, Oncotarget 7 (2016), https://doi.org/10.18632/oncotarget.12003.
[41] N. Ruiz-Lafuente, A. Minguela, A. Parrado, DOCK9 induces membrane ruffles and Rac1 activity in cancer HeLa epithelial cells, Biochem. Biophys. Rep. 14 (2018) 178–181, https://doi.org/10.1016/j.bbrep.2018.05.004.
[42] K. Kurokawa, R.E. Itoh, H. Yoshizaki, Y.O.T. Nakamura, M. Matsuda, Coactivation of Rac1 and Cdc42 at lamellipodia and membrane ruffles induced by epidermal growth factor, Mol. Biol. Cell 15 (2004) 1003–1010, https://doi.org/10.1091/mbc.e03-08-0609.
[43] J. Mikuła-Pietrasik, P. Uruski, S. Szubert, D. Szpurek, S. Sajdak, A. Tykarski, K. Książek, Malignant ascites determine the transmesothelial invasion of ovarian cancer cells, Int. J. Biochem. Cell Biol. 92 (2017) 6–13, https://doi.org/10.1016/j.biocel.2017.09.002.
[44] L. Pascual-Antón, B. Cardeñes, R. Sainz de la Cuesta, L. González-Cortijo, M. López-Cabrera, C. Cabañas, P. Sandoval, Mesothelial-to-Mesenchymal transition and exosomes in peritoneal metastasis of ovarian cancer, Int. J. Mol. Sci. 22 (2021) 11496, https://doi.org/10.3390/ijms222111496.
[45] D. Na, Z.-D. Lv, F.-N. Liu, Y. Xu, C.-G. Jiang, Z. Sun, Z.-F. Miao, F. Li, H.-M. Xu, Transforming growth factor beta1 produced in autocrine/paracrine manner affects the morphology and function of mesothelial cells and promotes peritoneal carcinomatosis, Int. J. Mol. Med. 26 (2010) 325–332.
[46] K. Ksiazek, J. Mikula-Pietrasik, K. Korybalska, G. Dworacki, A. Jörres, J. Witowski, Senescent peritoneal mesothelial cells promote ovarian cancer cell adhesion, Am. J. Pathol. 174 (2009) 1230–1240, https://doi.org/10.2353/ajpath.2009.080613.
[47] J. Mikuła-Pietrasik, P. Uruski, P. Sosińska, K. Maksin, H. Piotrowska-Kempisty, M. Kucińska, M. Murias, S. Szubert, A. Woźniak, D. Szpurek, S. Sajdak, K. Piwocka, A. Tykarski, K. Książek, Senescent peritoneal mesothelium creates a niche for ovarian cancer metastases, Cell Death Dis. 7 (2016) e2565, https://doi.org/10.1038/cddis.2016.417, e2565.
[48] J. Mikuła-Pietrasik, P. Uruski, M. Pakuła, K. Maksin, S. Szubert, A. Woźniak, E. Naumowicz, D. Szpurek, A. Tykarski, K. Książek, Oxidative stress contributes to hepatocyte growth factor-dependent pro-senescence activity of ovarian cancer cells, Free Radic. Biol. Med. 110 (2017) 270–279, https://doi.org/10.1016/j.freeradbiomed.2017.06.015.
[49] K.L. Sodek, K.J. Murphy, T.J. Brown, M.J. Ringuette, Cell-cell and cell-matrix dynamics in intraperitoneal cancer metastasis, Cancer Metastasis Rev. 31 (2012) 397–414, https://doi.org/10.1007/s10555-012-9351-2.
[50] L. Carduner, J. Leroy-Dudal, C.R. Picot, O. Gallet, F. Carreiras, S. Kellouche, Ascites-induced shift along epithelial-mesenchymal spectrum in ovarian cancer cells: enhancement of their invasive behavior partly dependant on αv integrins, Clin. Exp. Metastasis 31 (2014) 675–688, https://doi.org/10.1007/s10585-014-9658-1.
[51] I. Matte, C.M. Legault, P. Garde-Granger, C. Laplante, P. Bessette, C. Rancourt, A. Piché, Mesothelial cells interact with tumor cells for the formation of ovarian cancer multicellular spheroids in peritoneal effusions, Clin. Exp. Metastasis 33 (2016) 839–852, https://doi.org/10.1007/s10585-016-9821-y.
[52] H.A. Kenny, C.-Y. Chiang, E.A. White, E.M. Schryver, M. Habis, I.L. Romero, A. Ladanyi, C.V. Penicka, J. George, K. Matlin, A. Montag, K. Wroblewski, S. D. Yamada, A.P. Mazar, D. Bowtell, E. Lengyel, Mesothelial cells promote early ovarian cancer metastasis through fibronectin secretion, J. Clin. Invest. 124 (2014) 4614–4628, https://doi.org/10.1172/JCI74778.
[53] K.M. Burleson, L.K. Hansen, A.P.N. Skubitz, Ovarian carcinoma spheroids disaggregate on type I collagen and invade live human mesothelial cell monolayers, Clin. Exp. Metastasis 21 (2004) 685–697.
[54] Y. Gao, R. Foster, X. Yang, Y. Feng, J.K. Shen, H.J. Mankin, F.J. Hornicek, M. M. Amiji, Z. Duan, Up-regulation of CD44 in the development of metastasis, recurrence and drug resistance of ovarian cancer, Oncotarget 6 (2015) 9313–9326, https://doi.org/10.18632/oncotarget.3220.
[55] R.A. Davidowitz, M.P. Iwanicki, J.S. Brugge, In vitro mesothelial clearance assay that models the early steps of ovarian cancer metastasis, J. Vis. Exp. (2012), https://doi.org/10.3791/3888.
[56] S.J. Hogg, J.J. Evans, P.H. Sykes, K. Chitcholtan, A method to investigate the anti-metabolic activity of anti-cancer agents on ovarian cancer cells cultured in a 96-well high throughput format, J. Ovarian Res. 8 (2015), https://doi.org/10.1186/s13048-015-0172-0.
[57] D. Loessner, A. Rockstroh, A. Shokoohmand, B.M. Holzapfel, F. Wagner, J. Baldwin, M. Boxberg, B. Schmalfeldt, E. Lengyel, J.A. Clements, D. W. Hutmacher, A 3D tumor microenvironment regulates cell proliferation, peritoneal growth and expression patterns, Biomaterials (2018) 190–191, https://doi.org/10.1016/j.biomaterials.2018.10.014, 63–75.
[58] V.W. van Hinsbergh, A. Collen, P. Koolwijk, Role of fibrin matrix in angiogenesis, Ann. N. Y. Acad. Sci. 936 (2001) 426–437, https://doi.org/10.1111/j.1749-6632.2001.tb03526.x.

[59] Q. Gao, Z. Yang, S. Xu, X. Li, X. Yang, P. Jin, Y. Liu, X. Zhou, T. Zhang, C. Gong, X. Wei, D. Liu, C. Sun, G. Chen, J. Hu, L. Meng, J. Zhou, K. Sawada, R. Fruscio, T. W. Grunt, J. Wischhusen, V.M. Vargas-Hernández, B. Pothuri, R.L. Coleman, Heterotypic CAF-tumor spheroids promote early peritoneal metastatis of ovarian cancer, J. Exp. Med. 216 (2019) 688–703, https://doi.org/10.1084/jem.20180765.

[60] K.M. Nieman, I.L. Romero, B. Van Houten, E. Lengyel, Adipose tissue and adipocytes support tumorigenesis and metastasis, Biochim. Biophys. Acta BBA - Mol. Cell Biol. Lipids 1831 (2013) 1533–1541, https://doi.org/10.1016/j.bbalip.2013.02.010.

[61] K.M. Nieman, H.A. Kenny, C.V. Penicka, A. Ladanyi, R. Buell-Gutbrod, M. R. Zillhardt, I.L. Romero, M.S. Carey, G.B. Mills, G.S. Hotamisligil, S.D. Yamada, M. E. Peter, K. Gwin, E. Lengyel, Adipocytes promote ovarian cancer metastasis and provide energy for rapid tumor growth, Nat. Med. 17 (2011) 1498–1503, https://doi.org/10.1038/nm.2492.

[62] A. Ladanyi, A. Mukherjee, H.A. Kenny, A. Johnson, A.K. Mitra, S. Sundaresan, K. M. Nieman, G. Pascual, S.A. Benitah, A. Montag, S.D. Yamada, N.A. Abumrad, E. Lengyel, Adipocyte-induced CD36 expression drives ovarian cancer progression and metastasis, Oncogene 37 (2018) 2285–2301, https://doi.org/10.1038/s41388-017-0093-z.